Characterization of a novel laboratory internal recycle reactor for HTFT studies

By

Hema Vallabh

Submitted in partial requirement of the requirements for the degree of

Master of Science in Engineering

April 2008

Centre for Catalysis Research

Department of Chemical Engineering

University of Cape Town

Synopsis

This study aims to fully characterise the Stirred from Top Internal Recycle Reactor (STIRR) by means of a residence time distribution (RTD) study to determine its suitability for catalyst testing for High Temperature Fischer-Tropsch studies. It is required to not only ensure that the reactor behaves as a perfectly mixed CSTR, and but also to confirm that there is indeed sufficient flow through the catalyst bed thus ensuring adequate gas-catalyst contact.

An experimental programme was designed to determine the recycle ratio within the reactor and to prove that there is undoubtedly flow through the catalyst bed. Nitrogen and hydrogen were used as feed gases and methane as the inert tracer. A flexible capillary was used as the inlet and outlet for the reactor.

The experimental study was performed in two parts, the first being the method development study which involved the refinement of the RTD method to ensure that the system was indeed operating correctly before the specific characterization experiments could be carried out.

Due to the rapid dispersion of the methane tracer into the feed gases, thereby preventing the recycle peaks from being resolved, a novel method of placing the inlet and outlet capillaries in close proximity to each other was established to overcome this problem.

Once the reactor was performing satisfactorily, the second part of the experimental study, the reactor characterization, was performed. The effect of temperature, pressure, catalyst mass, syngas composition and recycle flow under Fischer-Tropsch conditions was investigated. Both nitrogen and hydrogen feed gases were used.

Recycle peaks for hydrogen, however, could only be distinguished at a temperature of 25℃. At temperatures above this, the methane tracer recycle peaks could not be detected. All remaining studies were performed using nitrogen feed gas.

Based on the findings, the following conclusions were drawn. Firstly, the positioning of the capillary is imperative in determining the recycle ratios. Secondly, there is sufficient recycle flow within the reactor which is associated with flow through the catalyst bed thereby ensuring adequate gas-catalyst contact. Finally, sufficient recycle flow is achieved under HTFT conditions making the reactor suitable for HTFT catalyst testing.

Acknowledgements

I would like to acknowledge my sponsors Sasol and the NRF for their financial support without which this project would not have been possible.

I'd like to express my sincere thanks to my supervisor, Prof Jack Fletcher. Thank you for your guidance and support throughout the period of this project, and for taking the time to go through the painstaking process of dotting the i's and crossing the t's in my thesis.

To Roald Brosius, for all his assistance with this project, from construction of the reactor test unit, conduction of experiments, and up to and including the compiling of this thesis, I am immensely grateful for your help. I would also like to thank Frans Prinsloo from Sasol R&D for his mentorship and assistance with this project. Thank you for always being so willing to help and for always remaining so involved with the project.

Thanks must also be extended to everyone who assisted in the laboratory, especially Shaun Cawood and Marc Wüst. Thank you for providing the man-power required to tighten those nuts and bolts. To Herman, thank you for all the work done on my rig and for always seeing to any repairs or modifications with a smile on your face.

I would also like to extend a general thanks to all the members of the Centre for Catalysis Research. Thank you to my colleagues who provided an entertaining work environment which helped me get through those stressful times.

Finally, I would like to thank my parents, family and friends for their continuous confidence in my ability to progress this far with my studies. Knowing that I have their support, I can only go from strength to strength.

Table of contents

Synopsis ..... **i**

Acknowledgements ..... **ii**

Table of contents ..... **iii**

List of figures ..... **vi**

List of tables ..... **ix**

List of Symbols ..... **x**

Glossary ..... **xii**

1. Introduction **1**

2. Literature Review **2**

2.1 Overview of laboratory scale reactors 2

2.2 Recycle reactors 4

2.2.1 Carberry reactor 5

2.2.2 Jet loop recycle reactor 5

2.2.3 Berty reactor 6

2.2.4 Modified 'Berty' reactor 7

2.3 Internal flow in a mechanically stirred recycle reactor 9

2.3.1 Influence of the impeller on the work done on the fluid in the reactor 9

2.3.2 Influence of viscosity and pressure drop on the flow through the catalyst bed 12

2.4 Reactor characterization 14

2.4.1 Performing a heat balance as a means to calculate recycle ratios 14

2.4.2 Residence time distribution studies 16

2.4.3 Quantifying recycle ratios 18

2.4.4 Qualitative determination of the degree of mixing in the reactor 20

2.4.5 Axial dispersion model 21

3. Objectives of Study **23**

4. Experimental **24**

4.1 Experimental apparatus 24
4.1.1 Feed 24
4.1.2 Reactor 24
4.1.3 Reactor inlet and outlet 26
4.1.4 Pressure control 26
4.1.5 Methane tracer injection 27
4.1.6 RTD tracer response detection 27
4.1.7 Adaptations for FT runs 28
4.2 Catalyst 28
4.3 Experimental operating conditions 28
4.4 Experimental procedure for RTD studies 30
4.5 Experimental operating procedures 30
4.5.1 Catalyst loading 30
4.5.2 Capillary installation 30
4.5.3 Reactor operation 31
4.5.3.1 Start up procedure 31
4.5.3.2 Initiation of RTD experiments 32
4.5.3.3 Shut down procedure 32
4.6 RTD signal detection, analysis and data work-up 32
5. Residence time distribution study – Method refinement 34
5.1 Experimental 34
5.2 Results 36
5.2.1 Empty reactor 36
5.2.2 Single felt 38
5.2.3 Two felts 40
5.2.4 Change in position of outlet capillary 42
5.2.5 Reproducibility of results 44
5.3 Discussion 46
5.3.1 Conventional RTD experiments – Capillary position 1 46
5.3.2 Modified RTD experiments – Capillary position 2 47

6. Residence time distribution study – Reactor characterization.....50

6.1 Experimental.....50
6.2 Results.....52
6.2.1 Effect of pressure.....52
6.2.2 Effect of temperature.....55
6.2.3 Effect of catalyst mass.....57
6.2.4 Effect of syngas composition.....57
6.2.5 Recycle flow under HTFT conditions.....58
6.3 Discussion.....59
6.3.1 Effect of pressure, feed gas and temperature.....59
6.3.2 Effect of catalyst mass on recycle ratio.....62
6.3.3 Effect of syngas composition.....63
6.3.4 Recycle flow under HTFT conditions.....63

7. Conclusions.....65

References.....66

Appendix.....68

Appendix I – Pictures of reactor and reactor test unit.....68
Appendix II – Experimental lists.....72
Appendix III – Quadratic trend lines.....74
Appendix IV – Pressure drop calculations.....75

List of figures

Figure 2.1: Intergral or PFR model and design equation..... 2

Figure 2.2: Differential reactor model and design equation..... 3

Figure 2.3: Schematic showing PFR with external recycle..... 4

Figure 2.4: Internal view of the Carberry reactor..... 5

Figure 2.5: Jet Loop reactor concept..... 6

Figure 2.6: Internal view of Berty reactor..... 7

Figure 2.7. Internal view of Stirred from Top Internal Recycle Reactor (STIRR)..... 8

Figure 2.8: Velocity diagram of the internal flow and its influences within the reactor..... 11

Figure 2.9: Influnce of impeller speed on recycle flow (Prinsloo and Koning, 2005). 15

Figure 2.10: Schematic of flow through catalyst bed (Prinsloo and Koning, 2005)... 15

Figure 2.11: Ideal pulse injection tracer response in (a) PFR and (b) CSTR..... 17

Figure 2.12: Model showing plug flow with external recycle..... 18

Figure 2.13: FID trace showing decay of tracer pulse used to calculate recycle ratio..... 19

Figure 2.14: FID trace showing exponential decay of tracer to calculate mean residence time..... 20

Figure 4.1: PFD of reactor system..... 25

Figure 4.2: Schematic diagram of STIRR showing felts making up the catalyst bed (a) sintered metal felt (b) metal sieve plate upon which felt is placed.... 26

Figure 4.3: Schematic of two-way six port valve..... 27

Figure 4.4. PSD for spray-dried FT catalyst (a) before and (b) after sieving 28

Figure 4.5: Schematic representation of capillary positions..... 29

Figure 5.2: Typical tracer response in nitrogen feed gas in an empty reactor..... 36

Figure 5.3: Typical tracer response in hydrogen feed gas in an empty reactor..... 37

Figure 5.4: Recycle ratios obtained in empty reactor 37

Figure 5.5: Typical tracer response in nitrogen feed gas with 1 felt in place 38

Figure 5.6: Typical tracer response in hydrogen feed gas with 1 felt in place 39

Figure 5.7: Comparison of recycle ratios obtained in empty reactor and reactor with one felt* 39

Figure 5.8: Typical tracer response in nitrogen feed gas with 2 felts in place..... 40

Figure 5.9: Typical tracer response in hydrogen feed gas with 2 felts in place..... 41

Figure 5.10: Comparison of recycle ratios obtained in empty reactor, reactor with one felt and reactor with two felts 41

Figure 5.11: Typical tracer response in nitrogen feed gas with 2 felts in place and capillary in position 2 42

Figure 5.12: Typical tracer response in hydrogen feed gas with 2 felts in place and capillary in position 2 43

Figure 5.13: Comparison of recycle ratios obtained in empty reactor, reactor with one felt (Postion 1 and 2) and reactor with two felts (Postion 1 and 2)..... 43

Figure 5.14: Results of reproducibility study 44

Figure 5.15: Path of recycle loop (a) Capillary in position 1, (b) Flow of gas before first peak is detected (c) Complete recycle loop before second peak is detected 47

Figure 5.16: Path of recycle loop (a) Capillary in position 2, (b) Flow of gas before first peak is detected (c) Complete recycle loop before second peak is detected 48

Figure 6.1: Recycle ratio as a function of impeller speed and pressure – Hydrogen at T = 25℃..... 52

Figure 6.2: Recycle ratio as a function of impeller speed and pressure – Nitrogen at T = 25℃..... 53

Figure 6.3: Recycle ratio as a function of impeller speed and pressure – Nitrogen at T = 100℃..... 53

Figure 6.4: Recycle ratio as a function of impeller speed and pressure – Nitrogen at T = 200℃..... 54
Figure 6.5: Recycle ratio as a function of impeller speed and pressure – Nitrogen at T = 300℃..... 54
Figure 6.6: Recycle ratio as a function of impeller speed and temperature – Nitrogen at P = 10 bar 55
Figure 6.7: Recycle ratio as a function of impeller speed and temperature – Nitrogen at P = 20 bar 56
Figure 6.8: Recycle ratio as a function of impeller speed and temperature – Nitrogen at P = 30 bar 56
Figure 6.9: Effect of catalyst mass on recycle ratios 57
Figure 6.10: Effect of syngas composition on recycle ratios 58
Figure 6.11: Plot of pressure drop versus gas velocity (Nitrogen, T = 25℃)..... 61
Figure A1.1: Photograph of felt and metal sieve plate 68
Figure A1.2: Photograph of internal draft tube with felts and metal sieve plates 68
Figure A1.3: Photograph of reactor base, internal draft tube, felts and metal sieve plates 69
Figure A1.4: Photograph of reactor with internal draft tube in place showing catalyst neatly filling holes of metal sieve plate..... 69
Figure A1.5: Photograph of closed reactor with magnedrive impeller 70
Figure A1.6: Photograph of reactor base and lid with impeller..... 70
Figure A1.7: Photograph of reactor test unit 71
Figure A4.1: Velocity diagram of the internal flow and its influences within the reactor..... 76

List of tables

Table 2.1: Comparison of pulse and step inputs for RTD study 17

Table 4.1: Parameters investigated for experimental study 29

Table 5.1: List of experiments performed in method development study 34

Table 6.1: List of experiments performed in method development study 50

Table 6.2: Variation of the viscosity (μ) of hydrogen and nitrogen with temperature 61

Table 6.3: Change in pressure drop over catalyst bed with temperature for nitrogen 62

Table A2.1: Parameters investigated for experimental study 72

Table A2.2: List of experiments performed in method development study 72

Table A2.3: List of experiments performed in method development study 72

Table A4.1. Pressure drop calculation for nitrogen and hydrogen 75

List of Symbols

B_0	permeability co-efficient for viscous flow
c_i	concentration of species
c_p	heat capacity
D	mass diffusivity
F_0	initial mass flowrate
F_i	mass flowrate of species *i*
g	acceleration of gravity
H	enthalpy
k	thermal conductivity
$\dot{m}$	mass flowrate
L	characteristic length
P	pressure
Pe	Péclet number = $Re \cdot Sc$ (mass diffusion) or $Re \cdot Pr$ (thermal diffusion)
Pr	Prandtl number = $\frac{c_p \mu}{k}$
$\dot{Q}$	heat flow
q_0	volumetric flowrate
R	recycle ratio
r	specific reaction rate
Re	Reynold's number = $\frac{\rho v_s L}{\mu}$
Sc	Schmidt number = $\frac{\mu}{\rho D}$
t	time
t_r	theoretical residence time
T	temperature
T_{shaft}	torque
U	internal energy
u	velocity in the direction of the whirl
V	volume
V_{st}	volume of stirred tank
W_{cat}	catalyst weight
W_s	shaft work
X	conversion
x	coordinate direction
y	coordinate direction

z	coordinate direction
α	thermal diffusivity
v_s	mean fluid velocity
v	velocity components
μ	viscosity
ρ	density
ω	angular velocity

Glossary

CSTR	Continuous stirred tank reactor
HTFT	High temperature Fischer-Tropsch
GC	Gas chromatograph
FID	Flame ionization detector
FT	Fischer-Tropsch
STIRR	Stirred from top internal recycle reactor
JLR	Jet loop reactor
MFC	Mass flow controller
PFR	Plug flow reactor
PSD	Particle size distribution
RTD	Residence time distribution
sccm	Standard cubic centimetres per minute
SGHSV	Specific gas hourly space velocity

1. Introduction

Bench-scale reactors are used to study, test and develop catalysts for industrial scale catalyzed reactions such as the Fischer-Tropsch synthesis. It is desirable to perform such tests under conditions similar to commercial operation. This means that the absence of heat and concentration gradients is required to ensure that intrinsic reaction rates are measured which are needed for scale-up. One way to achieve this is to run a tubular reactor in differential reactor mode, making sure that the conversions are small so that the reaction rates can be considered reasonably constant. The major disadvantage is that this requires measuring a small concentration change in the feed. By introducing a recycle in the reactor setup, a high mass velocity through the catalyst, as encountered in commercial operating conditions, can be maintained independent of the feed rate. In this way, a net large concentration change is easily and accurately measured in the feed (Berty, 1976).

In recycle reactors at high recycle ratios, all gradients are minimized, even if not eliminated. The remaining gradients are small and calculable in reactors where the internal recycle flow can be measured (Berty, 1984). It can be shown that at the two extremes of zero and infinitely large recycle, a recycle reactor becomes a plug flow (PFR) and a well mixed (CSTR) reactor, respectively (Gillespie, 1966).

The well-defined flow path of the recycle reactors lends itself to an easy assessment of the recycle flow, while with CSTR's, the mixing can be perfect yet the contact between the catalyst and gas may still be poor or uncertain. There are various methods by which the recycle ratios can be determined. Indirectly, the recycle ratio can be obtained from the pressure drop over the catalyst bed or from the adiabatic temperature increase of the reacting gas passing through the catalyst (Berty, 1974). Both methods require either tedious calibrations or heat balance calculations respectively.

This paper presents an in depth literature survey on the aforementioned concepts and methods. It then goes on to discuss the results of the characterization of a laboratory internal recycle reactor and addresses the concern raised above that even though the gas may be well-mixed contact between gas and catalyst is uncertain.

2. Literature Review

2.1 Overview of laboratory scale reactors

Two common classes of bench-scale reactors are integral reactors, more commonly referred to as Plug Flow Reactors (PFR), and differential reactors.

In plug flow reactors, the reactants are constantly consumed as they flow down the length of the reactor (Figure 2.1). When modelling a PFR, it is assumed that the concentration varies continuously in the axial direction along the reactor. As a result, the reaction rate, which is a function of the concentration, will also vary axially. The design equation of an integral reactor, derived from first principles from the mole balance, is thus given as:

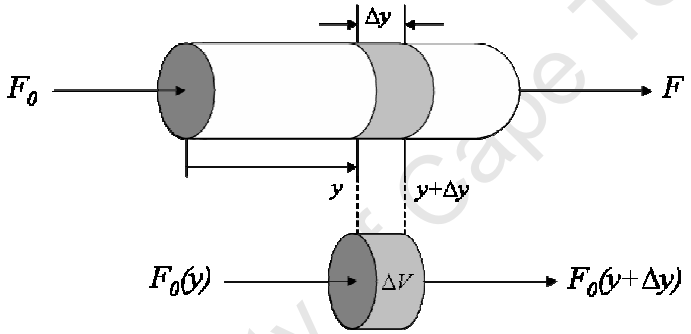

$$V = F_{A,0} \int_{X_{in}}^{X_{out}} \frac{dX}{-r_{eff}}$$

Figure 2.1: Intergral or PFR model and design equation

Laboratory plug flow reactors, while resembling industrial scale reactors in appearance, often cannot duplicate or, in some cases, even approximate the physical and chemical regime surrounding the catalyst in commercial operation (Berty, 1979). The presence of heat and concentration gradients in these reactors prevents the intrinsic rates, which are required for scale-up, from being measured. This is especially the case for fast reactions and even more so for exothermic reactions. As a means to largely overcome these difficulties, it is possible to operate a plug flow reactor in differential mode.

A differential reactor is one in which the conversion of reactants in the bed is limited and, consequently, so is the change is concentration though the bed. As a result, the reactant concentration though the reactor is essentially constant and approximately equal to the inlet

concentration - that is, the reactor is considered to be gradientless and the reaction rate is considered spatially uniform within the catalyst bed (Fogler, 1999). A diagrammatic representation of the differential reactor concept is shown in Figure 2.2 followed by the design equation derived from first principles.

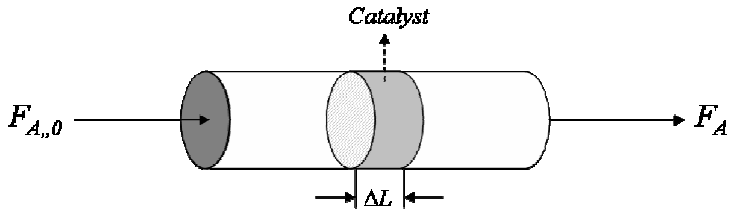

$$-r_{eff} = \frac{F_{A,0}\Delta X_A}{W_{cat}}$$

Figure 2.2: Differential reactor model and design equation

Operating a plug flow reactor in differential mode ensures that the conversions are kept low, thus allowing one to consider the reaction rates as reasonably constant. This method does, however, pose its own disadvantages, e.g. it requires measuring small concentration changes in a concentrated feed which leads to serious analytical errors and inaccuracy in the measurements. In order overcome this problem, continuously stirred tank reactors (CSTR) can be implemented.

A CSTR, or internally mixed reactor, ensures that the contents of the reactor are perfectly mixed and, as a result, reactions may be considered to take place at discharge conditions or very close to them. Like differential reactors, CSTR are gradientless reactors and, hence, the rates are measured directly and can be used for accurate scale up in commercial reactor design.

The basic principle of the CSTR is that it is essentially a reactor in which reacting fluid is circulated at a very high rate, thereby ensuring that the concentration of the fluid being circulated is the same as that of the effluent stream. As fresh feed enters through the inlet stream, it is diluted by the vast excess of the agitated fluid already in the reactor at some concentration C_0. This essentially means that with each internal cycle, as the feed fluid enters the reactor it is converted to a sufficient extent to maintain the contents of the reactor at concentration C_0 (i.e. a differential conversion of feed fluid occurs). Based on this viewpoint, the behaviour obtained in a well mixed reactor such as the CSTR can be achieved by means other than employing fluid stirring within the vessel. The alternative is the recycle reactor (Carberry, 1964).

2.2 Recycle reactors

Recycle reactors are essentially plug flow reactors with recycle, either internal or external (Figure 2.3). When the recycle is extremely high, the conversion per pass is small and the reactor can be treated as a differential reactor (Levenspiel, 1972). By introducing a large but finite recycle, all gradients are sufficiently minimized if not completely eliminated. Any remaining gradients are small and can be discounted (Berty, 1984).

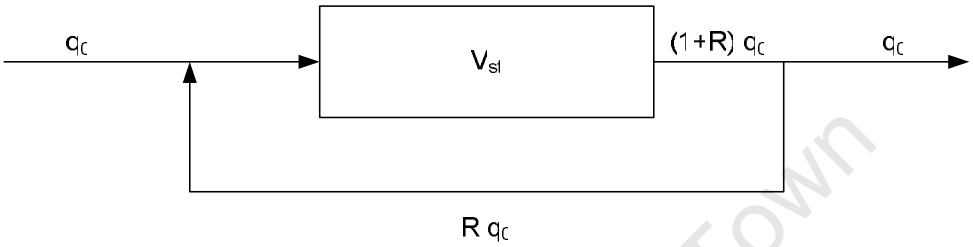

Figure 2.3: Schematic showing PFR with external recycle

The fact that with sufficient recycle heat and mass transfer conditions can be achieved similar to those in commercial operation, allows for the performance of the catalyst to be evaluated independently of the reactor performance. Furthermore, in industrial applications, the kinetic data obtained from recycle reactors can be used to design isothermal or adiabatic tubular reactors for production purposes, thus making it very attractive for catalyst development, testing and optimisation.

Recycle reactors fall under the class of CSTR and at recycle ratios greater than 20 behave as a perfectly mixed CSTR (Berty, 1974). Unlike laboratory tubular reactors which resemble commercial reactors in appearance but not in performance, recycle reactors conversely can mimic the chemical and physical regimes surrounding the catalyst in commercial reactors, but do not bear any resemblance in their physical appearance to such reactors.

There are, however, a few cases where recycle reactors are not recommended for laboratory studies, including when there is a possibility of homogenous reactions in the empty spaces of the reactor, and when there is a possibility of reaction taking place on the walls of the reactor due to the large wall surface to catalyst volume ratio in recycle reactors, as compared to tubular reactors (Berty, 1984).

Despite these limitations, recycle reactors are still the most promising means of performing catalytic testing on a laboratory scale. There are a number of recycle reactors available, each having their own unique design, operation and of course their own set of advantages and disadvantages for specific uses.

2.2.1 Carberry reactor

The Carberry reactor was designed by James Carberry and co-workers as an internal recycle reactor for experimental studies in the determination of the kinetics of gas/solid catalytic reactions (Carberry et al, 1980)

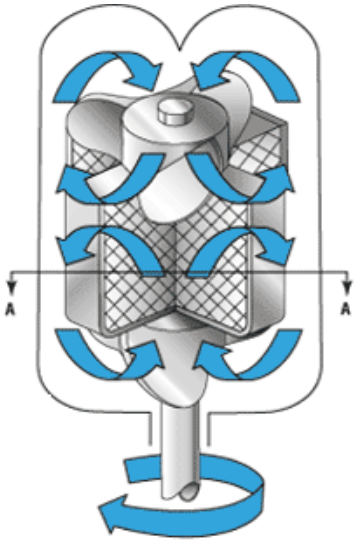

Figure 2.4: Internal view of the Carberry reactor

As can be seen in Figure 2.4, the Carberry reactor has four catalyst baskets each attached to a rotating central shaft. Impellers, both at the top and bottom of the shaft, increase the mixing and direct the flow of the fluid. Catalyst particles are placed in a catalyst basket which sweeps through the gases at high speeds, similar to the case in commercial operation, and thereby allows for sufficient gas-catalyst contact. The high level of mixing is achieved by the rotational velocity of the shaft (and basket) and the feed rate which ensure that the reactor performance can be likened to that of a CSTR (Carberry, 1964).

The reactor boasted the advantage of performing experiments in an isothermal environment and at overall conversion levels that can be easily measured. The reactor is particularly well suited to heterogeneous catalytic investigations.

2.2.2 Jet loop recycle reactor

The jet loop reactor, designed by Luft in the late 1960's, may be classified as a recycle reactor. Unlike the Carberry reactor, the jet loop recycle reactor does not employ mechanical mixing and internal mixing is achieved by a venturi effect of the high gas velocity through an

inlet jet or nozzle (Shermuly and Luft, 1977), thereby creating a recycle stream through the draft tube within the reactor as can be seen in Figure 2.5. This design was modified by Möller et al. (1995) to over come the bed channelling problems experienced with the original design.

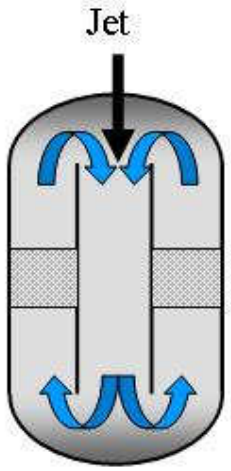

Figure 2.5: Jet Loop reactor concept

The major advantage of jet loop reactors over traditional recycle reactors is that is has no moving parts. Most recycle reactors have complex internal structures and impellers which require regular maintenance and potentially lead to problems at high temperatures and pressures. Furthermore, the jet loop reactor can be constructed from quartz thereby making it extremely useful for reactions promoted by stainless steel such as the methanol to olefins reaction. On the other hand, the primary disadvantage of the jet loop reactor is that high recycle ratios are limited by the maximum jet head pressure attainable (Möller et al, 1995)

A modified jet loop reactor was comprehensively characterized by Schwan (2001) to assess the influence of various parameters such as temperature, geometry of the nozzle, friction in the catalyst bed, flow rate and catalyst particle size on the recycle ratio. A residence time distribution study demonstrated the reactor's approximation of an ideally mixed reactor (CSTR) with negligible concentration and temperature gradients. Results from these studies showed that the minimum friction in the nozzle and the catalyst bed was achieved at low temperatures resulting in increasing recycle ratios with decreasing temperatures. The recycle ratios were also found to decrease with decreasing catalyst particle size and decreasing flow rate.

2.2.3 Berty reactor

This internal recycle catalytic reactor was developed by Union Carbide and built by Autoclave Engineers in the 1970's to perform catalyst testing and kinetic studies under conditions

mimicking those on a commercial scale. This extremely well mixed recycle reactor, with negligible temperature and concentration gradients, ensures heat and mass transfer conditions similar to those in the actual commercial units. This was a major breakthrough as it allowed for catalyst development and testing to be conducted on laboratory scale, while still being directly applicable to commercial scale (Berty, 1974).

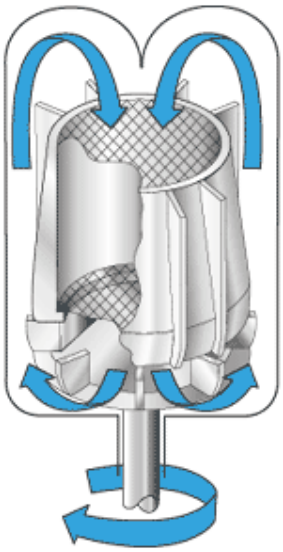

Figure 2.6: Internal view of Berty reactor

With regards to the design, the Berty reactor has a catalyst basket positioned directly above an impeller directing fluid as shown in Figure 2.6. The catalyst basket is made up of two sintered metal felts which serve as the floor and ceiling of the catalyst basket. However, during Fischer-Tropsch catalyst testing studies performed in industry using the Berty reactor, it was found that an accumulation of catalyst particles and heavier hydrocarbons in the bearings of the impeller shaft led to mechanical problems and ultimately failure of the magnedrive (Prinsloo and Koning, 2005), and similar problems have become commonplace amongst the user fraternity of these reactor types.

2.2.4 Modified 'Berty' reactor

This modified reactor is based on the design of the original Berty reactor. It operates in the same manner as the Berty reactor, with the major difference being the position of the impeller shaft (Figure 2.7). In the new, improved design, the impeller is inverted and driven from the top of the reactor to prevent mechanical problems arising to the accumulation of catalyst particles in the bearings of the magnedrive. Depending on whether the impeller is spun in a

clockwise or anti-clockwise direction, the gas flow is either sucked through the bed (as shown in figure 2.7), or conversely pushed through the bed respectively.

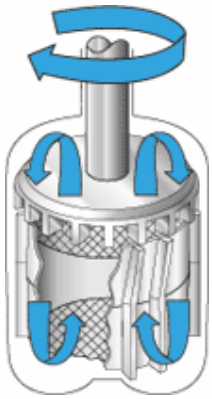

Figure 2.7. Internal view of Stirred from Top Internal Recycle Reactor (STIRR)

Like in the original design of the Berty reactor, this modified reactor, which is hereafter referred to as the Stirred from Top Internal Recycle Reactor (STIRR), contains a thin catalyst bed in the centre of the reactor. In theory, this recycle reactor should behave like a CSTR due to the high internal recycle ratio within the reactor.

The STIRR boasts a number of advantages over the original Berty reactor, viz.

- As already mentioned, the most important advantage is the prolonged lifetime of the Magnedrive impeller. This ensures that the reactor operates smoothly for longer periods and also reduces maintenance costs.
- The modified reactor is smaller and hence easier to handle during loading and removal of catalyst.
- Heating and cooling times of the reactor are reduced due to the modified reactor being smaller that than the original Berty reactor.
- The modified reactor is more robust and reliable.

Limited studies have however been performed on the characterization of this reactor system.

2.3 Internal flow in a mechanically stirred recycle reactor

2.3.1 Influence of the impeller on the work done on the fluid in the reactor

In order to obtain a sufficiently high degree of recycle flow within the reactor, it must be ensured that the internal mixing within the reactor is satisfactory. In the case of the STIRR, recycle flow is achieved mechanically by an internal impeller. This impeller is required to drive gas through the catalyst basket in order to obtain sufficient gas-catalyst contact and create an internal recycle flow path for the gas. The catalyst bed itself offers resistance to flow thereby requiring a driving force to push gas through the bed. This driving force is provided by the pressure drop generated over the catalyst bed, which of course varies depending on the gases utilised.

In order to overcome the problem incurred by the resistance to the flow, it is imperative to analyse the source of the pressure drop generated to overcome this problem. Keeping in mind that the impeller is the primary means by which the gas flow within the reactor is obtained, it is appropriate to consider the relationship between the velocity head provided by the impeller and the pressure drop required to push gas through the catalyst bed. In steady state operation, the velocity head generated by the impeller is equal to the velocity head that produces the flow through the catalyst bed.

The pressure drop over the catalyst is generated by the impeller. This relationship can be analysed using the principle of thermodynamics of an open system. A general energy balance for a control volume can be constructed as the basis (Smith, et al, 2005). In the STIRR, the control volume is chosen such that it encompasses the impeller but not the catalyst basket. According to the first law of thermodynamics, energy is conserved. As a result, the rate of change of energy within the control volume equals the net rate of energy transfer into the control volume as is described in the modified energy balance shown in Equation 2.1.

$$\frac{d(mU)_{cv}}{dt} = -\Delta\left[\left(U + \frac{1}{2}u^2 + zg\right)\dot{m}\right]_{fs} + \dot{Q} + \textit{work rate} \qquad \text{(Equation 2.1)}$$

The left hand side of the equation represents the rate of accumulation term. Work is associated with the moving of flowing streams in and out of the control volume. The fluid at the entrance and exit of the control volume has an average set of properties which include *temperature, pressure, enthalpy, energy,* etc. A unit mass of fluid at the entrance is acted upon by additional fluid exerting a constant pressure P. The work done in moving the unit mass through the entrance is *PV*, and the work rate is $(PV)\dot{m}$. Because "Δ" denotes the difference between exit and entrance quantities, the net work done *on* the system is given by

$-\Delta[(pV)\dot{m}]_{fs}$. Another form of work is shaft work indicated by rate $\dot{W}_s$ and if the control volume doesn't expand or contract as is the case here, it is the only other form of work done on the system. Now if one introduces these terms into Equation 2.1, combining the definition of enthalpy, $H = U + pV$, Equation 2.1 can be written as:

$$\frac{d(mU)_{cv}}{dt} + \Delta\left[\left(H + \frac{1}{2}u^2 + zg\right)\dot{m}\right]_{fs} = \dot{Q} + \dot{W}_s \qquad \text{(Equation 2.2)}$$

For flow processes, steady state is defined by the fact that the accumulation in the system is zero. At steady state, no changes in the properties of the fluid within the control volume occur nor at its entrance or exit. The resulting equation is the mathematical expression of the first law of thermodynamics for a steady state flow process between one entrance and one exit. All terms represent energy per unit mass of fluid. Equation 2.2 can then be simplified to:

$$\Delta H + \frac{\Delta u^2}{2} + g\Delta z = Q + W_s \qquad \text{(Equation 2.3)}$$

If one neglects potential energy changes and assumes that this is a reversible adiabatic (isentropic) process, then the equation further reduces to:

$$W_s = \int V dP + \frac{\Delta u^2}{2} \qquad \text{(Equation 2.4)}$$

For reversible adiabatic compression, the following holds:

$$dH = c_p dT = \int V dP \qquad \text{(Equation 2.5)}$$

which is equivalent to $PV^{\gamma} = cte$ (Equation 2.6)

Work done on the system is applied to increase the enthalpy and the kinetic energy of the flow. The enthalpy relates to an increased temperature and static pressure from the work done on the gas in the tangential direction (Bathie, 1984). The increase in the kinetic energy arises from the work done in the axial direction. The stagnation temperature, i.e. total temperature, of a flowing fluid is defined as the temperature that would result if the fluid would be brought to rest adiabatically and reversibly. This temperature rise is of course accompanied by a further rise of pressure. The stagnation enthalpy increase then gives rise to a stagnation pressure increase from the contributing enthalpy and kinetic energy rise:

$$H_t = H + \frac{v^2}{2} \qquad \text{(Equation 2.7)}$$

Furthermore, the rate of energy transfer for a rotor in the tangential direction is the product of the torque and the angular velocity. Thus,

$$P = \omega T_{shaft} = \dot{m}\left(\omega r_2 v_{u_2} - \omega r_1 v_{u_1}\right) \quad \text{(Equation 2.8)}$$

Since

$$u = \omega r$$

the rate of energy transfer becomes

$$P = \omega T_{shaft} = \dot{m}\left(u_2 v_{u_2} - u_1 v_{u_1}\right) \quad \text{(Equation 2.9)}$$

or per unit mass

$$W_{\tan} = \left(u_2 v_{u_2} - u_1 v_{u_1}\right) \quad \text{(Equation 2.10)}$$

where v_{u_1} and v_{u_2} are the velocity components in the direction of the whirl u. A velocity diagram of the impeller speed, the absolute gas v_1 and v_2 and the gas velocities relative to the blade of the impeller w_1 and w_2 can be viewed in Figure 2.8.

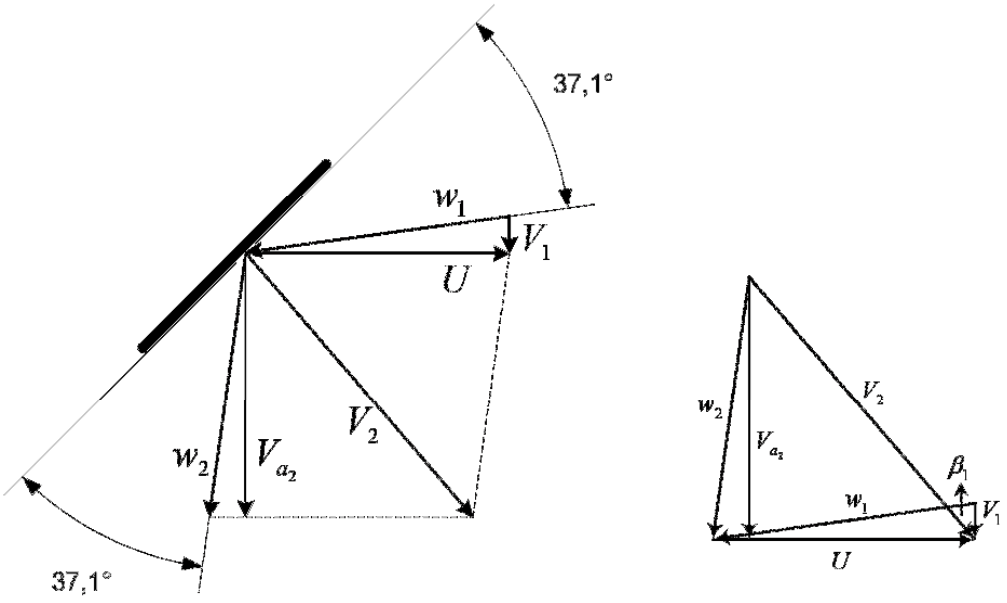

Figure 2.8: Velocity diagram of the internal flow and its influences within the reactor

The work done on the gas in an axial direction per unit mass of fluid is then given by:

$$W_{axial} = \frac{v_{a_2}^2}{2} - \frac{v_{a_1}^2}{2} \qquad \text{(Equation 2.11)}$$

Combining W_{tan} and W_{axial} gives W_s. Thus the total work done on the gas can be calculated from the impeller speed and the gas velocity.

2.3.2 Influence of viscosity and pressure drop on the flow through the catalyst bed

As aforementioned, the generated velocity head driving the gas through the catalyst bed equals the velocity head offered by the resistance to flow through the bed. The latter is far more difficult to calculate with any reasonable degree of accuracy. The results can, however, be qualitatively explained using the empirical and fundamental principles of gas flow through porous media. The basic law governing permeability calculations for laminar, viscous flow is given by Darcy's Law. This law states that the linear gas velocity is directly proportional to the pressure gradient causing flow. If Δp is small compared to p, the following holds:

$$u = -\frac{B_0}{\mu}\frac{\partial p}{\partial x} = \frac{B_0}{\mu}\frac{\Delta P}{L} \qquad \text{(Equation 2.12)}$$

where B_0 is the permeability co-efficient for viscous flow

The change from laminar to turbulent flow should occur in porous media with an increase of flow rate (Carman, 1956). Resistance due to eddy formation can be described as inertial resistance and depends on the kinetic energy per unit volume of the fluid, i.e. on ρu^2. The simplest assumption is to regard inertial resistance as superimposed on the viscous resistance. Thus,

$$\frac{\Delta P}{L} = au + bpu^2 \qquad \text{(Equation 2.13)}$$

$$\text{with } a = \frac{\mu}{B_0}$$

If the pressure drop is plotted against the gas velocity, the slope of the linear regression curve is related to the viscosity which is invariant with pressure and permeability. If the curves are plotted for various pressures and the slopes vary with pressure then it can be said that B_0

depends on pressure. Thus, from equation 2.12, it can be deduced that the effect of pressure, which now influences both terms in the numerator, would be greater than the effect of viscosity.

Understanding the basis behind the internal flow in the reactor enables one to determine the driving force through the catalyst bed and the dominating parameters which influence flow through the bed.

2.4 Reactor characterization

An ideally mixed reactor system is required for investigations into FT catalyst performance tests. In order to ensure that this regime exists within the system, the reactor needs to be characterised so as to verify that CSTR performance as well as adequate recycle is indeed achieved.

Calculating the recycle ratio within the reactor allows one to determine the behaviour of the system. According to Gillespie and Carberry (1966), a recycle ratio greater than 20 is sufficient to approximate the performance of a CSTR. Two common practices for calculating recycle ratios are the use of a heat balance and by means of a residence time distribution (RTD) study.

2.4.1 Performing a heat balance as a means to calculate recycle ratios

In order to determine flow through the catalyst bed and, hence, calculate the recycle ratio within the reactor, a heat balance may be carried out over the reacting system. This is effected by recording temperature measurements above and below the catalyst bed, and thereafter by calculating the adiabatic temperature rise the recycle ratio can be obtained. The following equations apply:

$$\Delta T_{bed} = \frac{\Delta T_{ad}}{R} \qquad \text{(Equation 2.14)}$$

$$\Delta T_{ad} = \frac{c_0 \Delta H_r}{\rho c_p} X \qquad \text{(Equation 2.15)}$$

where ΔT_{bed} is the temperature difference measured across the catalyst bed in K, c_0 is the concentration of reactant in kg/m^3, ΔH_r is the enthalpy of reaction in J/g.mol, c_p is the heat capacity of the gas mixture in J/g.K and X is the conversion. These equations are valid for systems in which the gas velocity and the properties of the gas are independent of conversion (Berty, 1974).

A study implementing this method was performed by Prinsloo and Koning (2005) in order to characterise the STIRR. Results from the study and which pertain to the determination of the recycle ratios are presented in Figure 2.9.

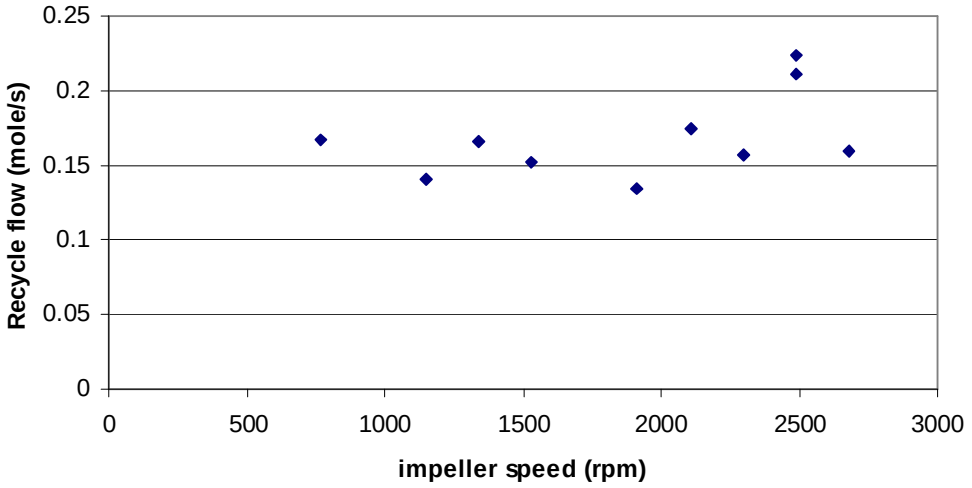

Figure 2.9: Influnce of impeller speed on recycle flow (Prinsloo and Koning, 2005)

As is evident from Figure 2.9, the apparent invariance in recycle flow (and hence recycle ratio) with increasing impeller speeds suggested this method to be inadequate in practice and was attributed possibly to experimental difficulties in obtaining measured temperature differences.

The temperature difference across the catalyst bed is measured by placing thermocouples above and below the catalyst bed, as can be seen in Figure 2.10. It must, however, be noted that the method is likely only to be accurate if the gas flow pattern within the reactor is as shown in Case 1 of Figure 2.10. If the flow dynamics is better represented by that of Case 2 in Figure 2.10, the temperature measured at T_1 is in fact incorrect as it then measures gas that has already been in contact with the catalyst bed. T_1 is hence overestimated in this case. As a result the temperature difference (T_2-T_1) will be very small, in turn, resulting in a large recycle ratio.

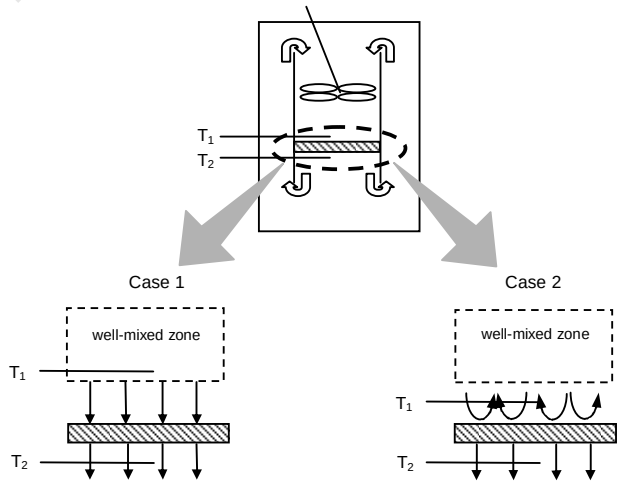

Figure 2.10: Schematic of flow through catalyst bed (Prinsloo and Koning, 2005)

Furthermore, despite the fact that the findings of Prinsloo and Koning (2005) indicated the recycle ratios to be sufficiently high as to represent CSTR behaviour in the modified Berty reactor, the fact that no direct relationship between the impeller speed and recycle ratios could be established raises the question as to whether there is indeed adequate flow through the catalyst bed and not merely intense mixing in the reactor without true recycle flow.

It may thus be concluded from his study that further characterization is necessary to determine the effect of impeller speed on the mixing (and, indeed, recycle ratio) achieved in the STIRR.

2.4.2 Residence time distribution studies

The use of residence time distributions to analyse flow within chemical reactors was first explored in the 1930's by MacMullin and Weber (1935). Later, in the 1950's, the subject was further extended to be more applicable to systems of interest by Danckwerts (1953). It has since been used extensively in characterizing flow in chemical reactors.

The residence time distribution of a reactor is a characteristic of the mixing that occurs within the reactor – it provides valuable information about the system and is generally considered to be one of the most informative characterization tools for chemical reactors (Fogler, 1999).

In order to measure the RTD of a reactor system, an inert material or tracer needs to be injected into the reactor at a known time $t=0$. The introduction of the tracer should not affect the flow pattern within the system. The concentration of the tracer is then measured in the effluent stream at time $t > 0$, and the response is analysed to determine the RTD of the system. It is imperative that the tracer has the following characteristics:

- Stable and conserved (non-reactive) so that it can be accounted for by material balance
- Experimentally distinguishable from fluid being studied
- Analysis should be convenient, sensitive and reproducible
- Physical properties similar to that of the reaction mixture
- Completely soluble in the mixture
- Should not absorb on or react with the surface of the vessel
- Inexpensive and easy to handle

These characteristics ensure that measurement of the tracer response of the effluent stream is a true reflection of the overall fluid flow pattern through the reactor. Various methods of

introducing the tracer exist, however, the two most widely applied are the pulse input and step input methods.

In the pulse input experiment, a known amount of tracer is rapidly injected into the reactor feed stream, in a single dose as quickly as possible. For the step input experiment, an instantaneous change in the tracer inlet concentration is made from an initial steady state level (usually zero) to a second level. This concentration of tracer in the feed is kept at a constant level until the concentration of the tracer in the effluent is indistinguishable from that in the feed (Fogler, 1999).

Table 2.1: Comparison of pulse and step inputs for RTD study

	Advantages	**Disadvantages**
Pulse input	Requires small amount of tracer	Difficult to achieve perfect pulse input
	Small impact on process operation	Difficult to achieve accurate mass balance on tracer
Step input	Easier to achieve	Continuous delivery requires greater amount of tracer
	More accurate mass balance on tracer is obtainable	May have significant effect on process operation

(Fogler, 1999)

A typical pulse input injection and response is shown in Figure 2.11 for both an ideal PFR and CSTR. For an ideal PFR, the response is a spike of infinite height and infitesimal width (Figure 2.11a), whereas in the case of a CSTR, the response is made up of a sharp peak and a tail with exponential decay (Figure 2.11b). However, in reality the idealized responses of Figure 2.11 rarely present.

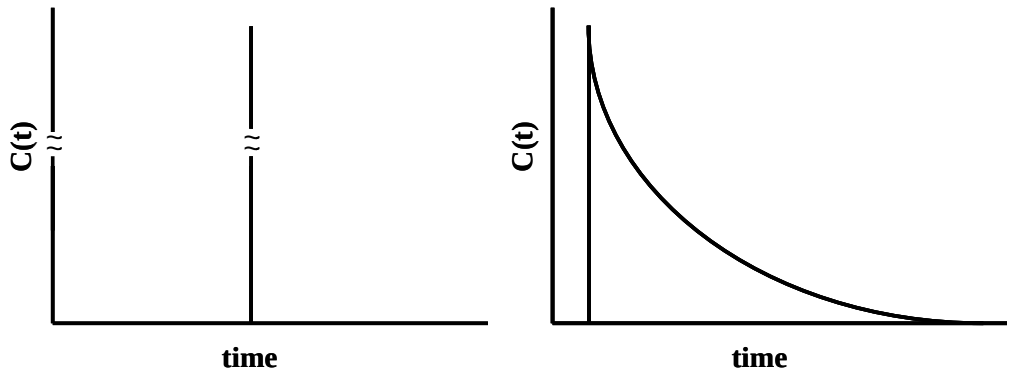

(a) (b)

Figure 2.11: Ideal pulse injection tracer response in (a) PFR and (b) CSTR

2.4.3 Quantifying recycle ratios

The RTD of a recycle reactor can be mathematically modelled as a plug flow reactor with external recycle as shown in Figure 2.12.

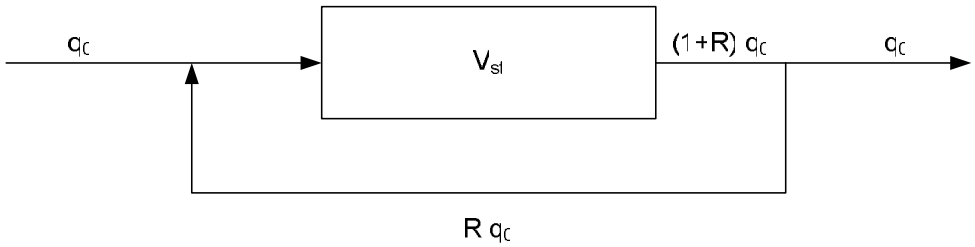

Figure 2.12: Model showing plug flow with external recycle

According to Rippin (1967), the time taken for a single pass through the recycle reactor shown in Figure 2.12 is given by

$$\frac{V_{st}}{(1+R)q_0} = \frac{t_r}{(1+R)}$$

where q_0 is the flowrate, R is the recycle ratio and t_r is the theoretical residence time for the pulse to pass through the reactor. Consider an amount $q_o \Delta t$ of material entering the system at between time $t=0$ and Δt. All this will reach the exit of the reactor at time $\frac{t_r}{(1+R)}$, but a fraction $\frac{R}{(1+R)}$ is returned in the recycle, so that the amount leaving the system with age $\frac{t_r}{(1+R)}$ is $\frac{q_0 \Delta t}{(1+R)}$ and the fraction in the outlet with the same age is $\frac{1}{(1+R)}$. The recycle material passes through the reactor again and on reaching the reactor exit for the second time its age is $\frac{2t_r}{(1+R)}$. The fraction if this material in the outlet stream is then $\frac{1}{(1+R)}\left(\frac{R}{(1+R)}\right)$. After i passages through the reactor, the material's age is $\frac{it_r}{(1+R)}$ and the fraction of this material in the exit stream is $\frac{1}{(1+R)}\left(\frac{R}{(1+R)}\right)^{i-1}$. The RTD will thus

consist of an infinite series of impulses (delta functions) spaced at intervals of $\frac{t_r}{(1+R)}$ and whose magnitude decreases as a geometric series given by

$$f(t) = \sum_{i=1}^{\infty} \frac{1}{1+R}\left(\frac{R}{1+R}\right)^{i-1} \delta\left(t - \frac{it_r}{1+R}\right) \qquad \text{(Equation 2.16)}$$

With no recycle, the only non-zero term of the series is the first and this gives the single impulse at time $t = t_r$, which is the RTD of a PFR. It can also be shown that when R is large, the RTD for a CSTR reduces to $\frac{1}{t_r} e^{\left(\frac{-t}{t_r}\right)}$ (Rippin, 1967). At intermediate recycle, the recycle ratio can be calculated using the time interval between peaks of the tracer effluent response.

Figure 2.13 represents a typical GC trace obtained from a RTD study using a pulse input. The recycle peaks are clearly visible.

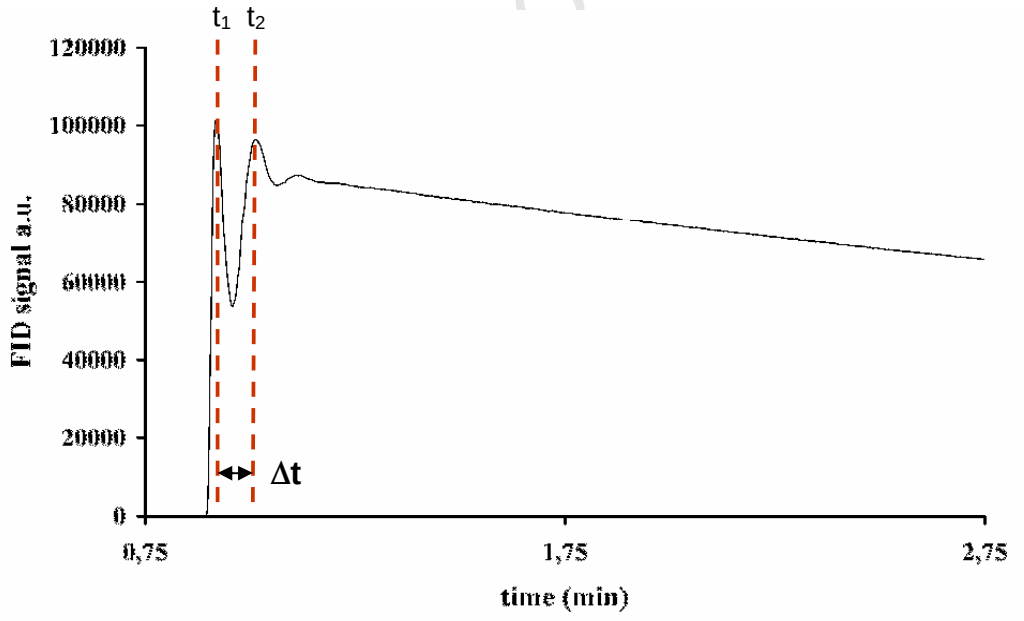

Figure 2.13: FID trace showing decay of tracer pulse used to calculate recycle ratio

Based on the aforementioned model and related equations, using the time interval between peaks, the recycle ratio may then be calculated as follows:

$$R = \frac{t_r}{\Delta t} - 1 \qquad \text{(Equation 2.17)}$$

where $t_r = \frac{V_{st}}{q_0}$, and

$$\Delta t = t_2 - t_1 \qquad \text{(Equation 2.18)}$$

The degree of mixing within the reactor may be then be quantified by using the value obtained for the recycle ratio.

From a practical perspective, the early tracer response is of importance since, at later times, pulse dispersion into the feed gas makes it impossible to discern the recycle peaks and, consequently, the recycle ratio can no longer be determined. Nonetheless, this method is still preferred as it allows one to directly quantify the recycle ratios and, hence, the effect of reactor operating variables on flow and mixing within the reactor.

2.4.4 Qualitative determination of the degree of mixing in the reactor

Another method for evaluating CSTR performance makes use of the mean residence time. The mean residence time is calculated from the response of the tracer pulse input and thereafter compared to the theoretical residence time to determine the extent of mixing in the system. This method is usually implemented when the dispersion of the tracer into the feed gas occurs so rapidly that the recycle peaks can no longer be clearly distinguished and, hence, cannot be used to directly calculate the recycle ratio.

Figure 2.14 presents a typical FID response of a pulse input tracer with rapid diffusion of the tracer into the feed gas.

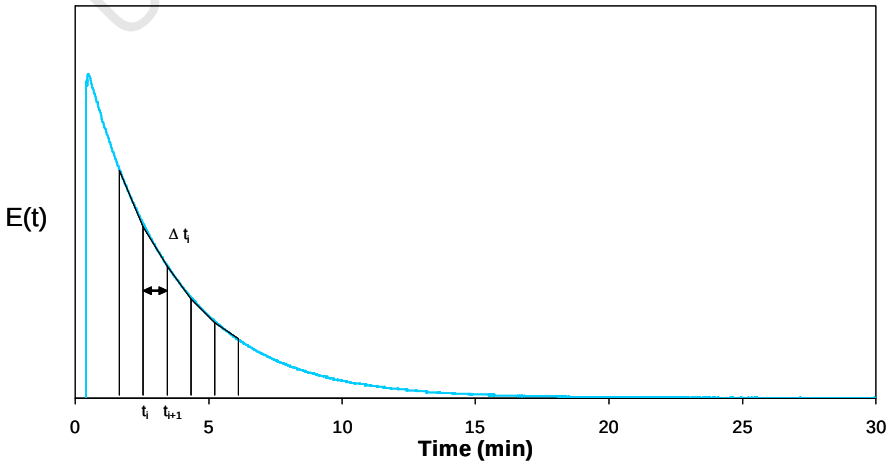

Figure 2.14: FID trace showing exponential decay of tracer to calculate mean residence time

The mean residence time can be determined by calculating the area under the tracer response curve using the following equations.

$$\bar{t}_{r,calc} = \sum_{i}^{n_C=1} \left[t_i^2 E(t)_{av} \Delta t_i \right]_{av} \Delta t_i \qquad \text{(Equation 2.19)}$$

where

$$E(t) = C(t) = \frac{c_i(t)}{\int_0^\infty c_i(t)dt} \qquad \text{(Equation 2.20)}$$

The theoretical residence time is defined as the ratio of the volume of the reactor to the volumetric flow rate entering the reactor. Hence, for a perfectly mixed reactor,

$$t_{r,calc} = t_r = \frac{V_{st}}{q_0} \qquad \text{(Equation 2.21)}$$

Thereafter, the experimental mean residence time is compared to the theoretical mean residence time. If the calculated and theoretical mean residence times correspond, it can be concluded that the system is in fact displaying CSTR behaviour.

The advantage of this method is that the extent of mixing can be quantitatively determined even if the dispersion of the tracer into the feed gas occurs too rapidly for the tracer recycle peaks to be evident on the tracer response curve. However, the method does not enable any quantification of the recycle ratio. Results are obtained in the form of a qualitative deviation from ideal mixing.

This method is used as a qualitative means to ensure a system is well mixed when a comprehensive characterization of a reactor system is not practicable.

2.4.5 Axial dispersion model

An axial dispersion model can be developed to describe the residence time distribution of a reactor and is particularly suited to systems approaching PFR behaviour. The model is then used to simulate a reactor RTD study thereby enabling one to fully characterise the mixing properties of the reactor.

Voncken, Holms and den Hertog (1964) modelled the loop reactor with a dispersion model and proposed a solution for the case of complete recirculation. Mathur and Weinstein (1980)

considered partial recirculation and developed expressions for the moments of the RTD. The common model parameters include the recycle ratio and the Péclet number, also commonly referred to as the Bodenstein number.

The Péclet number (Pe) is a dimensionless number relating the rate of flow advection to its rate of diffusion. It is equivalent to the product of the Reynolds number (Re) and the Prandtl number (Pr) in the case of thermal diffusion, and the product of the Reynolds number with the Schmidt number (Sc) in the case of mass diffusion. The definitions of the Péclet number for both cases are presented mathematically as follows:

Thermal diffusion:

$$Pe_L = \frac{Lv}{\alpha}$$
$$Pe_L = \mathrm{Re}_L \cdot Pr$$

Mass diffusion:

$$Pe_L = \frac{Lv}{D}$$
$$Pe_L = \mathrm{Re}_L \cdot Sc$$

Where L is the characteristic length, v is the velocity, α is the thermal diffusivity $\alpha = \frac{k}{\rho c_p}$ (made up of thermal conductivity (k), density (ρ), heat capacity (c_p)) and D is the mass diffusivity.

When the Péclet number approaches zero, the behaviour of the axial dispersion model approaches the behaviour of a continuous stirred tank reactor model. At the other extreme, when the Péclet number approaches infinity, the behaviour of the axial dispersion model approaches the behaviour of a plug flow reactor model (Melo et al., 2001).

3. Objectives of Study

The Stirred from Top Internal Recycle Reactor represents a novel design modification to the conventional Berty internal recycle reactor. However, before this reactor can be implemented for catalytic studies, the operation and characteristics of the STIRR first need to be fully explored. To date, the internal recycle within this reactor has been only incompletely studied by Prinsloo and Koning (2005) and, hence, the mixing and recycle characteristics of the reactor are still to be determined.

This study aims to fully characterise the reactor by means of a residence time distribution study to determine its suitability for catalyst testing under HTFT conditions. It is required to not only ensure that the reactor behaves as a perfectly mixed CSTR, and but also to confirm that there is indeed sufficient gas-catalyst contact. Moreover, keeping in mind that in order for an internal recycle reactor to be classified as a CSTR, recycle ratios of greater than 20 need to be obtained. The effect of various operating variables such as pressure, temperature, catalyst mass and feed gas composition, on the recycle ratio will be investigated to ensure that under the intended Fischer-Tropsch use conditions the recycle flow within the reactor is satisfactory.

4. Experimental

4.1 Experimental apparatus

Figure 4.1 presents a schematic diagram of the experimental apparatus constructed and used for this study. The reactor system consists of a Stirred from Top Internal Recycle Reactor (STIRR), followed by a back-pressure regulator for system pressurization. The reactor is preceded by a two-way, six port sampling valve used for methane tracer injection for the residence time distribution studies. A RTD response analysis is performed using a GC flame ionization detector (FID) coupled directly to the reactor effluent line (i.e. in place of the usual GC carrier gas line). A summary of the key components of the reactor system follows, including a brief description of their operation.

4.1.1 Feed

The gas flow was controlled and monitored by Brooks mass flow controllers. Flow rate was kept constant at 1500 sccm (standard cubic centimetre per minute), equivalent to standard Fischer-Tropsch synthesis operating conditions (SGHSV for 5 g catalyst). The feed gases – nitrogen, hydrogen and carbon monoxide (all pure gases) – were supplied via the laboratory lines, while methane was obtained from a high pressure gas cylinder.

4.1.2 Reactor

The STIRR is presented schematically in Figure 4.2. The reactor has a volume of 840 ml and is constructed of stainless steel. It comprises two parts, viz.

i. a 'lid' which is fixed through mounting to the test unit frame and to which is mounted the magnedrive and impeller assembly, and

ii. a 'body' which forms the internal flow path and includes a central draft tube and catalyst basket assembly. The internal draft tube holding the catalyst basket can be removed from the reactor for cleaning and catalyst reloading. The top of the catalyst basket consists of a wire mesh reinforced 15 μm sintered metal felt (hereafter referred to as a felt) (Figure 4.2a), which is placed upon a metal sieve plate with 5mm holes (Figure 4.2b) while the base of the basket consists of the metal sieve plate placed upon the felt. The impeller is driven in counter clockwise rotation by a

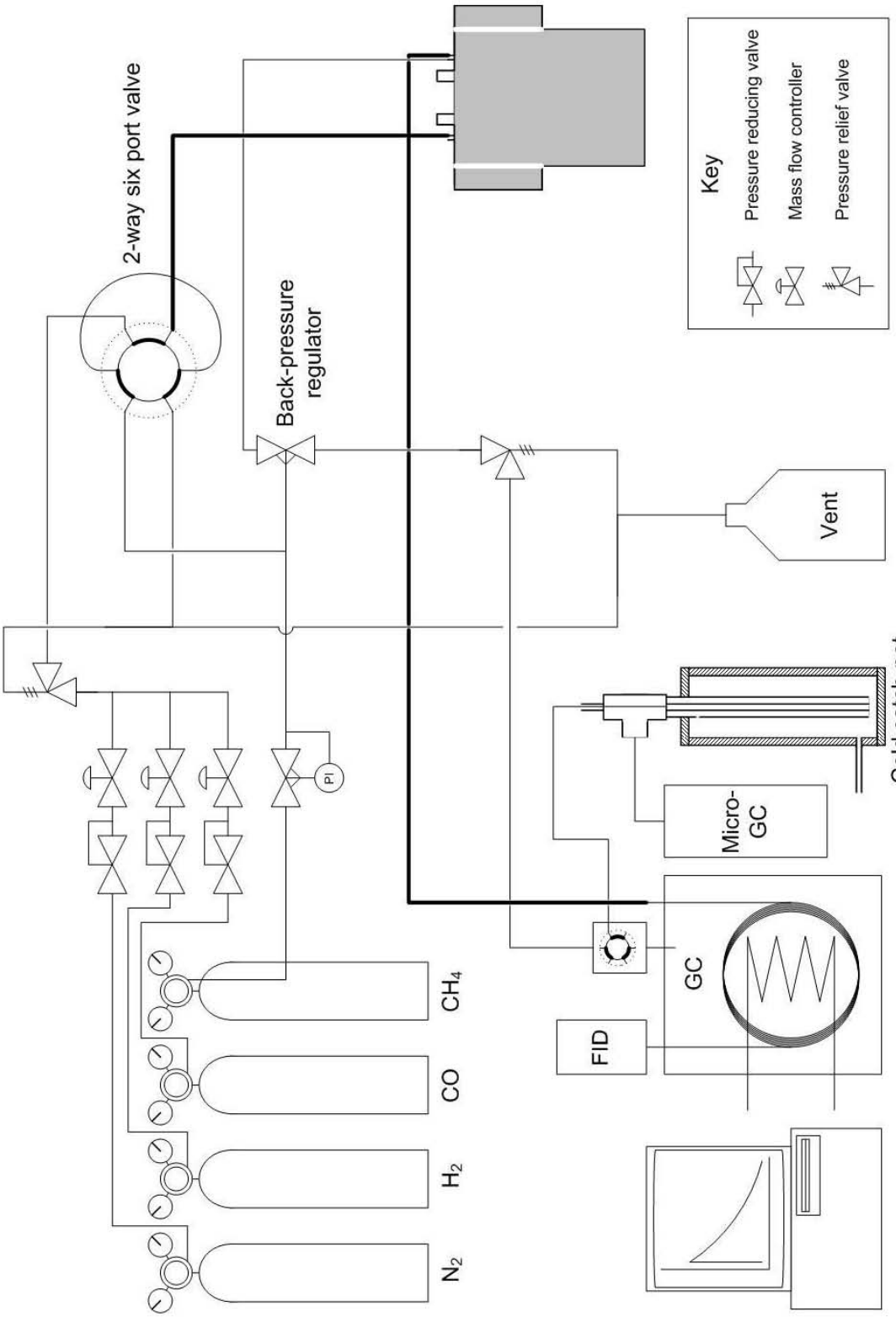

Figure 4.1: PFD of reactor system

variable speed motor (Bonfiglioli, 50 hertz, 0.55 kW) via the magnedrive, so that gas flow is downwards through the catalyst basket with recycle flow proceeding upwards external to the draft tube. The metal plate and felt assembly together serve as the ceiling and floor of the catalyst basket, ensuring that the catalyst does not escape from the basket into the reactor. Gas feed inlet and product outlet points are positioned in the reactor lid as indicated in Figure 4.2.

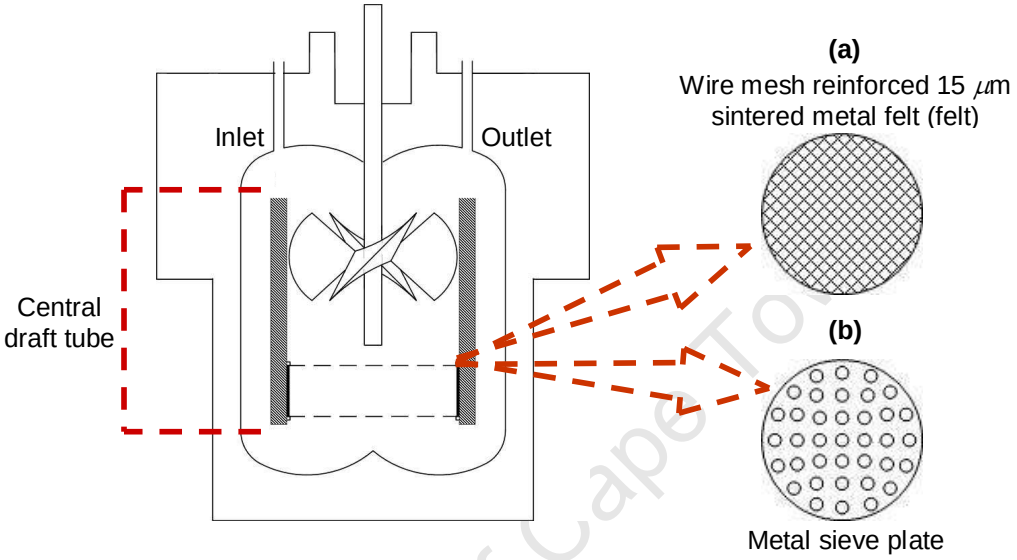

Figure 4.2: Schematic diagram of STIRR showing felts making up the catalyst bed (a) sintered metal felt (b) metal sieve plate upon which felt is placed

Pictures of the reactor and reactor test unit are presented in Appendix I.

4.1.3 Reactor inlet and outlet

A flexible capillary (15m VARIAN FactorFour, fused silica capillary, ID 0,25 mm) was used as the reactor inlet and outlet lines so as to reduce the dead volume outside of the reactor and consequently to reduce any tracer time lag between injection and detection. Furthermore, as determined experimentally, virtually no tailing of the input peak occurred. Thus the flow through the capillary is considered plug flow.

4.1.4 Pressure control

A dome-loaded diaphragm back-pressure regulator (0-750 psig, 52 bar rated at 300ºC, PEEK Seat, ¼ inch NPT fittings) is used to pressurise the reactor as required and is positioned after the reactor. Pressurized methane was used to set the back-pressure to the diaphragm and thereby pressurise the reactor.

4.1.5 Methane tracer injection

Methane pulses were injected into the reactor feed flow via an automated two-way high temperature and pressure gas sampling valve immediately upstream to the STIRR. The two-way six port valve was heated to 300℃ to ensure th at the valve mechanism was not damaged during operation.

A schematic of the valve is presented in Figure 4.3.

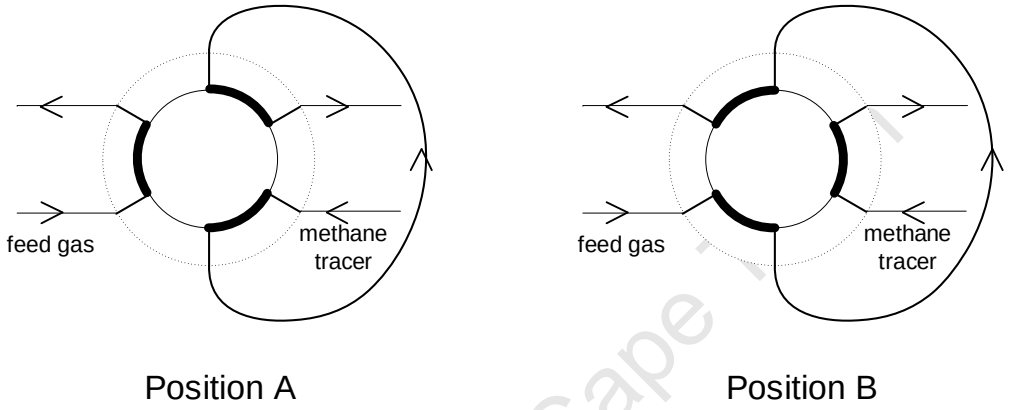

Figure 4.3: Schematic of two-way six port valve

When the valve is in position A, reactor feed gas flows through the valve directly to the reactor whilst, simultaneously, the methane tracer gas is flushed through the sample loop. In order to inject the methane pulse, the valve is switched into position B where the methane tracer in the sample loop is injected with the feed gas into the reactor. The valve is then returned to position A, where the sample loop is once again filled for the next injection. The valve was automated, actuating the methane pulse injection into the reactor.

4.1.6 RTD tracer response detection

All RTD tracer response detection was performed online using an FID detector associated with a VARIAN 3900 gas chromatograph with the reactor tracer effluent stream going directly to the FID as a carrier gas (i.e. the tracer effluent stream bypasses the normal GC injection column separation process). As a consequence of the automated injection (as per section 4.1.5) and data collection being synchronized, time lags were perfectly repeatable.

In order to limit the flow to the FID when the reactor was operated at high pressure (20-30 bar), to ensure that the FID flame was not blown out, multiple capillaries (up to 75m in total) for the outlet were connected in series between the reactor exit and the GC.

4.1.7 Adaptations for FT runs

Keeping in mind that the reactor was constructed for use in FT catalyst testing once fully characterized, the capillary outlet from the reactor is heated to a temperature of 150℃ using standard heating line. This is to ensure that the FT product, formed during catalyst testing, does not condense before reaching the GC.

4.2 Catalyst

A standard spray-dried iron Fischer-Tropsch catalyst was utilised for this study. The catalyst was sieved before use in the reactor so as to remove the fraction smaller than 25 μm. This ensures that the catalyst does not escape from the catalyst basket containing a 15 μm sieve. The particle size distribution (PSD) of the catalyst before and after sieving is presented in Figure 4.4. The apparatus used to obtain the PSD was a Malvern Mastersizer. The mean particle size of the catalyst applied was approximately 65 μm.

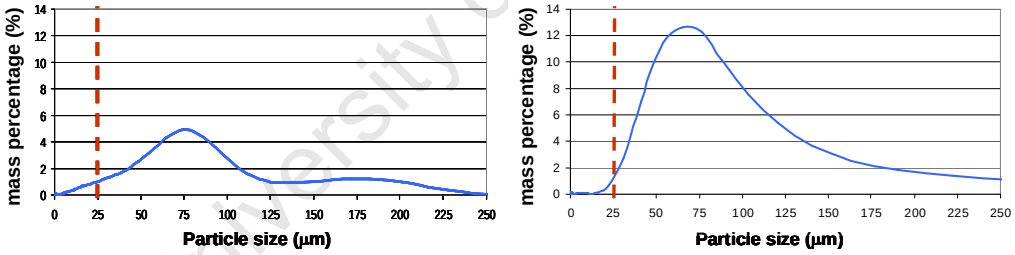

(a) (b)

Figure 4.4. PSD for spray-dried FT catalyst (a) before and (b) after sieving

This is the same catalyst that would be used in follow-up HTFT catalyst studies in the STIRR.

4.3 Experimental operating conditions

A number of experimental variables were investigated during the characterization of the STIRR. These include temperature, pressure, impeller speed, feed gas, internal configuration (i.e. resistance to flow) and inlet and outlet capillary position.

Table 4.1 shows the parameters that were investigated in the experimental RTD study for each experimental variable.

Table 4.1: Parameters investigated for experimental study

Gases	N_2
	H_2
	CO
Internal configuration	0 Felt
	1 Felt
	2 Felts
Capillary position*	Position 1
	Position 2
Temperature	25℃
	100℃
	200℃
	300℃
Pressure	10 bar
	20 bar
	30 bar

*The change in capillary position can be viewed in Figure 4.5.

Each of these parameters was tested at varying impeller speeds ranging from 250-2500 rpm. The gas flow rate was kept constant at 1500 sccm

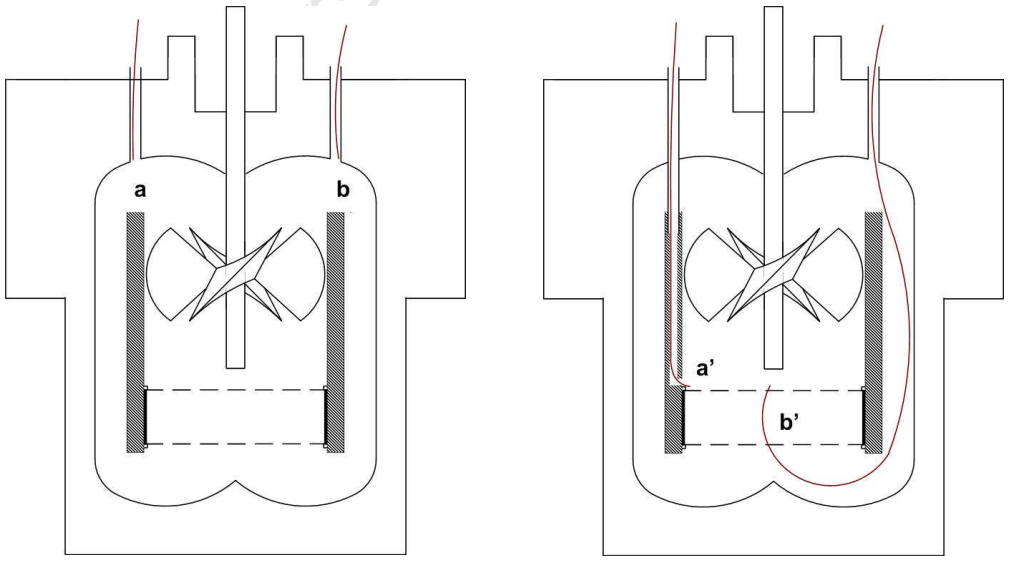

Figure 4.5: Schematic representation of capillary positions

4.4 Experimental procedure for RTD studies

The pulse injection method described in Section 2.4.2 was employed. An inert tracer, methane, is injected into the reactor at some time t=0. Once the tracer has entered the reactor, it is allowed to mix with the feed gas (hydrogen, nitrogen or syngas) before it exits the reactor at some time t >0 via the outlet capillary flowing directly to the GC-FID. Here the effluent tracer response is measured and its response analysed in order to calculate the reactor internal recycle ratio under each set of operating conditions.

For the purpose of this study, methane was utilised as the inert tracer using hydrogen, nitrogen and syngas (hydrogen and carbon monoxide mixtures) each as feed gasses in various experiments.

4.5 Experimental operating procedures

4.5.1 Catalyst loading

With the exception of experiments to investigate the effect of catalyst mass on recycle ratio, 5 g catalyst charge was used for each of the experiments. The catalyst is loaded by removing the internal draft tube containing the felts and metal sieve plates making up the catalyst basket. The metal sieve plate and bottom felt are tightened into position. The catalyst is spread evenly so that it fills the holes in the metal sieve plate. This ensures that the catalyst remains evenly spread over the bed during the experiments. The top felt and metal sieve plate are screwed into position after which the entire catalyst basket and draft tube assembly are placed into position in the reactor. For experiments where the inlet and outlet capillaries are placed in position 2, the capillaries are first put into position before the draft tube is inserted into the reactor.

4.5.2 Capillary installation

For the experiments conducted with the capillaries in position 1, the capillaries are positioned in the feed inlet and product outlet tubing in the reactor lid. For experiments performed with the inlet and outlet capillaries in position 2, however, the capillaries must be inserted into position before the draft tube is placed in the reactor by carefully extending it from its original position in the reactor lid and inserting it into the middle of the bottom felt, through the catalyst basket and finally through the top felt until it is approximately 1 cm above the top felt. The tip of the capillary is then snipped off to ensure that the tube is not blocked by any catalyst that

may have entered the capillary head. The capillary is then adjusted until it is approximately 3 mm above the top sieve.

The inlet capillary is also carefully extended from its original position and inserted into a hole drilled through the length of the wall of the draft tube until it is placed just above the top sieve (as shown in Figure 4.5).

Great care must be taken when positioning the capillaries as extensive bending and handling may cause the capillary to break. Once the catalyst is loaded and the capillaries are positioned correctly, the draft tube assembly is inserted into the reactor. While raising the reactor towards the reactor lid, the outlet capillary must be carefully monitored and adjusted so that it does not get caught between the reactor and the lid, which would cause it to break.

After the reactor lid is sealed, the reactor is ready for operation.

4.5.3 Reactor operation

4.5.3.1 Start up procedure

For experiments performed at room temperature and atmospheric pressure (25℃ and 1 atm), the feed gas and methane tracer valves are opened and the feed gas flow is set using the relevant MFC. The impeller speed is set to 720 rpm. After the conditions have settled in (by allowing a 30 minute waiting period) experiments are commenced.

For experiments run at elevated pressure, the reactor must first be pressurized. The impeller speed is set to 720 rpm and the shut-off valve to the inlet of the back-pressure regulator is opened. The pressure control gas (in this case, methane) is slowly bled in using the needle valve to raise the pressure in the back-pressure regulator. After reaching the desired pressure, both the inlet needle valve and the inlet shut-off valve are closed.

If the set pressure overshoots the desired pressure, the pressure in the back-pressure regulator is lowered until the desired pressure is reached. In order to lower the pressure, the outlet shut-off valve is opened and pressure in the back-pressure regulator is slowly released by opening needle valve. When the desired pressure is reached, both the needle valve and shut of valves are closed.

A pressure test is performed to ensure that there are no leaks in the system. This is done by setting the back-pressure regulator to 25 bar (using the above procedure), closing the methane shut-off valve and lowering the methane MFC setting to 0 %. The system is left in

this state for one hour. The test is successful if the pressure does not drop with more than 0.5 bar during this time.

If the pressure test is successful, the back-pressure regulator is set to the desired pressure. The feed gas valves are opened and the feed gas flow is set using the relevant MFC. The temperature is set to the desired set point and a time period of 30 minutes is allowed for the reactor to settle in. Thereafter experiments are commenced.

4.5.3.2 Initiation of RTD experiments

Once the experimental conditions have been set by the aforementioned procedure, the pulse injection command is entered into the system to proceed with the experiment. The experiment is run for the duration of the theoretical mean residence time of the methane tracer pulse. The experimental conditions are then adjusted for the next experiment and allowed 15 minutes to settle in. Thereafter, and the pulse injection procedure is repeated.

4.5.3.3 Shut down procedure

Once the experiments are completed, the reactor is shut-down by setting the temperature set point to 0°C. The reactor is de-pressurized to atmospheric pressure by letting the pressure down in a controlled manner using the needle valves on the back-pressure regulator. The impeller is switched off and the MFC setting of the feed gas is set to 0 %. The shut-off valves from the feed gas line and the methane line are closed. The reactor is left until it is completely cooled down.

4.6 RTD signal detection, analysis and data work-up

Simultaneous with tracer injection, the RTD response is recorded with time on stream and a typical tracer response curve is shown in Figure 4.6 in which the recycle peaks can be clearly discerned thus allowing for the calculation of the recycle ratios. The time interval between the first two peaks is calculated and used together with the theoretical mean residence time to calculate the recycle ratio.

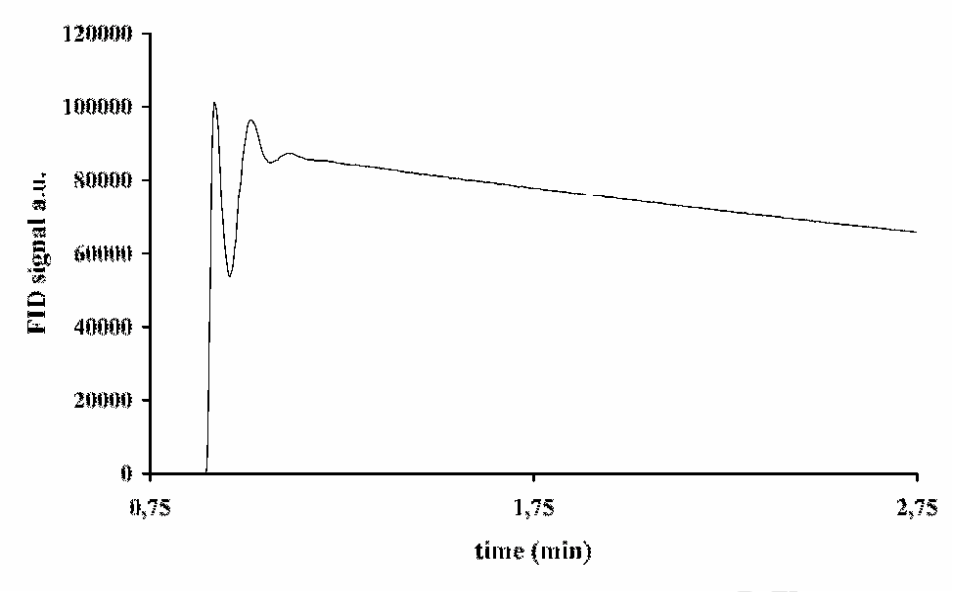

Figure 4.6: Initial period of typical GC trace magnified

As aforementioned, the pulse injection and data collection via the GC was automated to ensure uniformity in the experiments. The remote controlled sequence was set to run the GC for a period of 30 minutes. However, this is an overestimation of the time required for the tracer to travel through the reactor. Furthermore, only the initial period (approximately 2 minutes) of the trace is required for calculation of the recycle ratios as beyond this time any further tracer recycle peaks no longer distinguishable.

5. Residence time distribution study – Method refinement

5.1 Experimental

Initial residence time distribution experiments were performed in the reactor to ensure that the experimental system was indeed operating as expected before the specific characterization experiments could be carried out. The experimental study was designed such that the influence of each of the reactor's internal components, made up of two felts and two metal sieve plates together forming the floor and ceiling of the catalyst basket as described in Section 4.1.2, on the recycle flow within the reactor could be assessed. The first set of experiments was carried out in an empty reactor and thereafter the internal components were introduced one at a time.

Table 5.1 lists all experiments conducted in the method development study. A fold-out of the experimental lists can be found in Appendix II.

Table 5.1: List of experiments performed in method development study

Temperature: 25℃
Pressure: 10 bar
Gas flow rate: 1500 sccm

	Gas	Internal components	Capillary position
Exp 1	N_2	0 Felts	Position 1
Exp 2	H_2	0 Felts	Position 1
Exp 3	N_2	1 Felt	Position 1
Exp 4	H_2	1 Felt	Position 1
Exp 5	N_2	2 Felts	Position 1
Exp 6	H_2	2 Felts	Position 1
Exp 7	N_2	1 Felt	Position 2
Exp 8	N_2	2 Felts	Position 2
Exp 9	H_2	2 Felts	Position 2

For all experiments the impeller speed was varied from 720rpm – 2000rpm.

Experiments 1 and 2 were performed using nitrogen and hydrogen respectively as the feed gas flowing through an empty reactor. Thereafter, a single felt was placed in the reactor and the experiments were repeated in Experiments 3 and 4. After successfully completing the set of experiments with the single felt, the second felt was introduced and once again the

experiments were repeated (Experiments 5 and 6). Based on the results obtained from these experiments (to be discussed in Section 5.2), Experiments 3, 5 and 6 were repeated after changing the positions of the inlet and outlet capillaries (Experiments 1, 8 and 9).

The change in capillary position can be viewed in Figure 4.5.

5.2 Results

5.2.1 Empty reactor

The first set of experiments was performed in an empty reactor with no felts in place. Both nitrogen and hydrogen feed gases were investigated (in separate experiments – Exp 1 and Exp 2). Figures 5.2 and 5.3 show typical GC traces obtained for each of the feed gases from this set of experiments. It should be noted that in these experiments, tracer recycle peaks can be clearly discerned and, hence, the recycle ratios can be calculated by the method previously described in Section 2.4.3.

Figure 5.4 presents the recycle ratios obtained at different impeller speeds for each of the gases in an empty reactor. As is evident from Figure 5.4, for both feed gasses the recycle ratio increases monotonically with an increase in impeller speed. Furthermore, the recycle ratios obtained for nitrogen are higher than those obtained for hydrogen. The results presented in Figure 5.4 also show the measurability range within which the recycle ratios can be experimentally determined within a reasonable error.

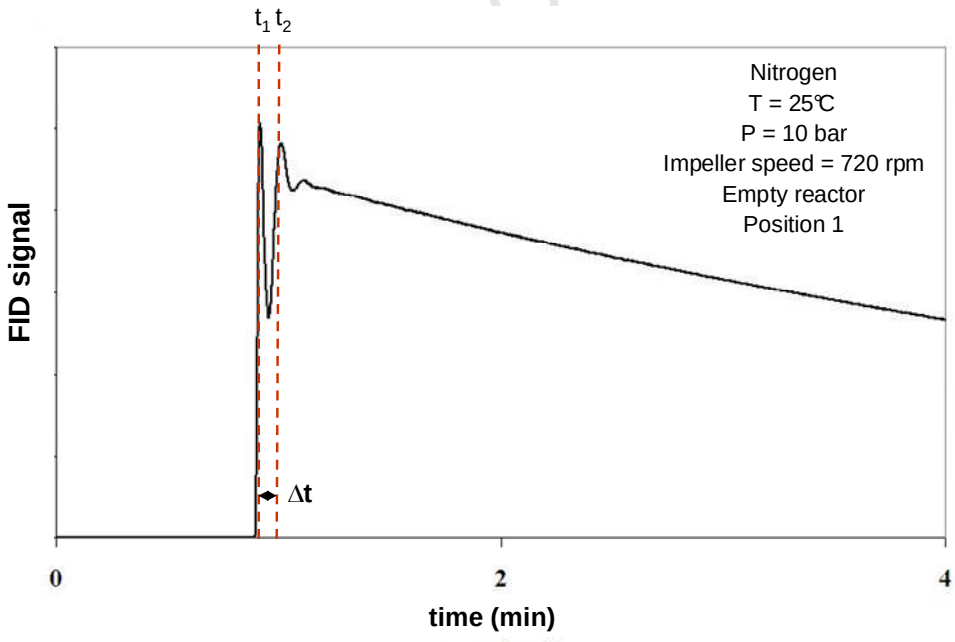

Figure 5.2: Typical tracer response in nitrogen feed gas in an empty reactor

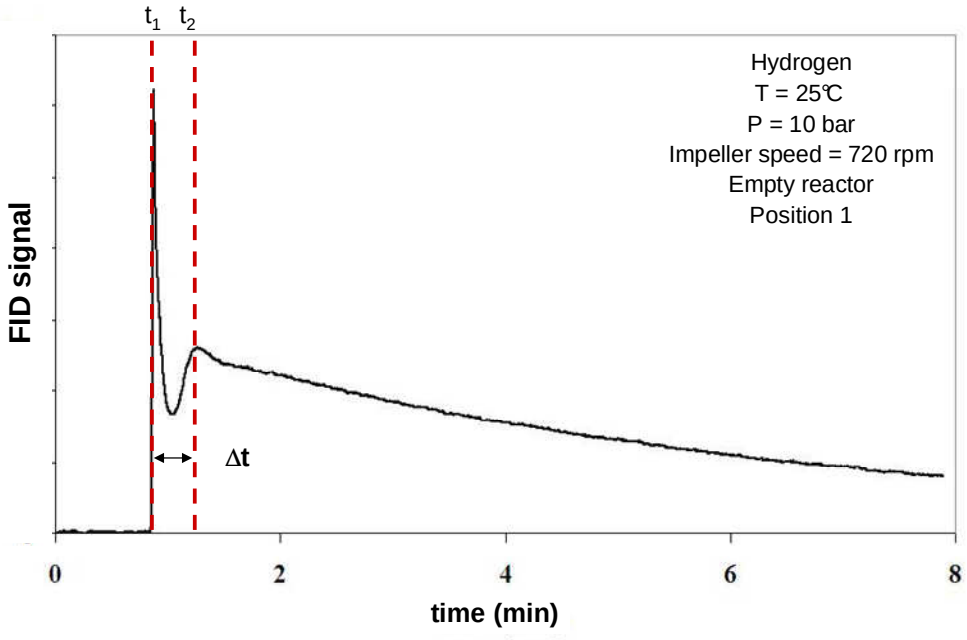

Figure 5.3: Typical tracer response in hydrogen feed gas in an empty reactor

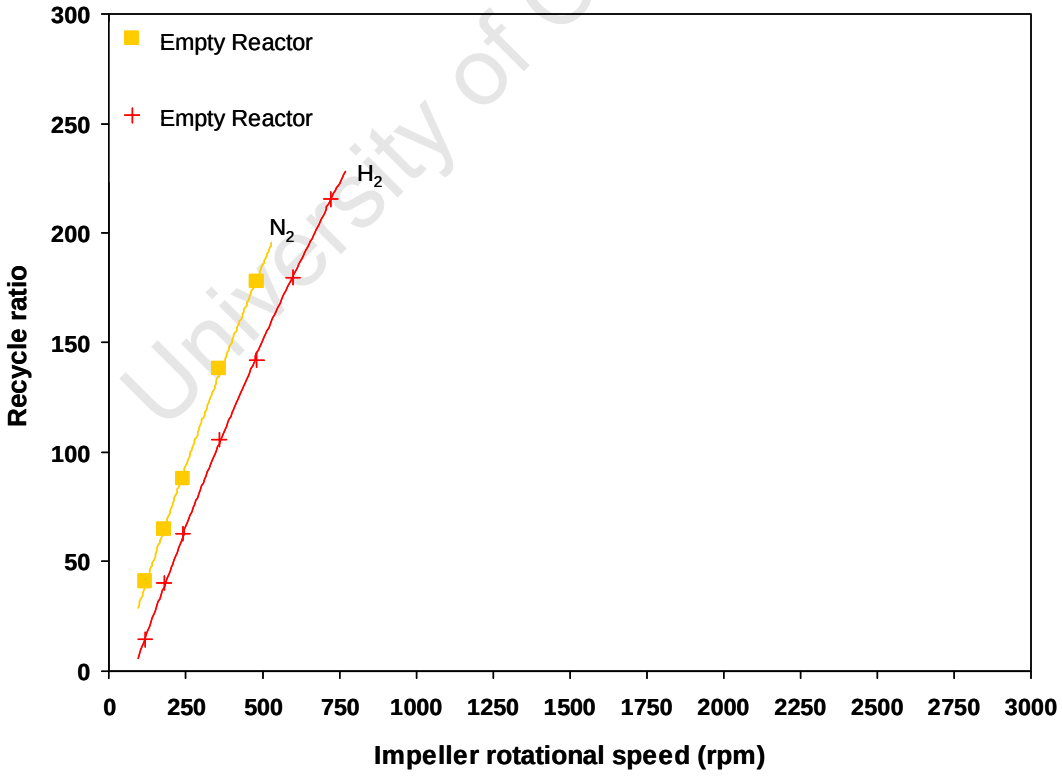

Figure 5.4: Recycle ratios obtained in empty reactor

5.2.2 Single felt

The next set of experiments was performed after placing a single felt in the reactor. This metal felt serves as part of the catalyst basket when the reactor is used to test catalytic reactions such as the FT synthesis. The metal felt offers resistance to the gas flow and is expected to affect the internal recycle ratio within the reactor. Typical tracer response curves obtained for each of the feed gases in this set of experiments are shown in Figures 5.5 and 5.6, respectively, followed by the effect on recycle ratio obtained with increasing impeller speed in Figure 5.7. The result is plotted on the same set of axes as those for the empty reactor, making the effect of the introduction of a single felt clear.

The most notable feature of the hydrogen feed gas experiment (Figure 5.6) is the absence of the second tracer recycle peak thereby making the calculation of the recycle ratios impossible, and consequently, such information is not presented in Figure 5.7. With regard to the nitrogen feed gas case, it can be seen that the increased resistance in flow within the reactor results in decreased recycle ratios, as expected.

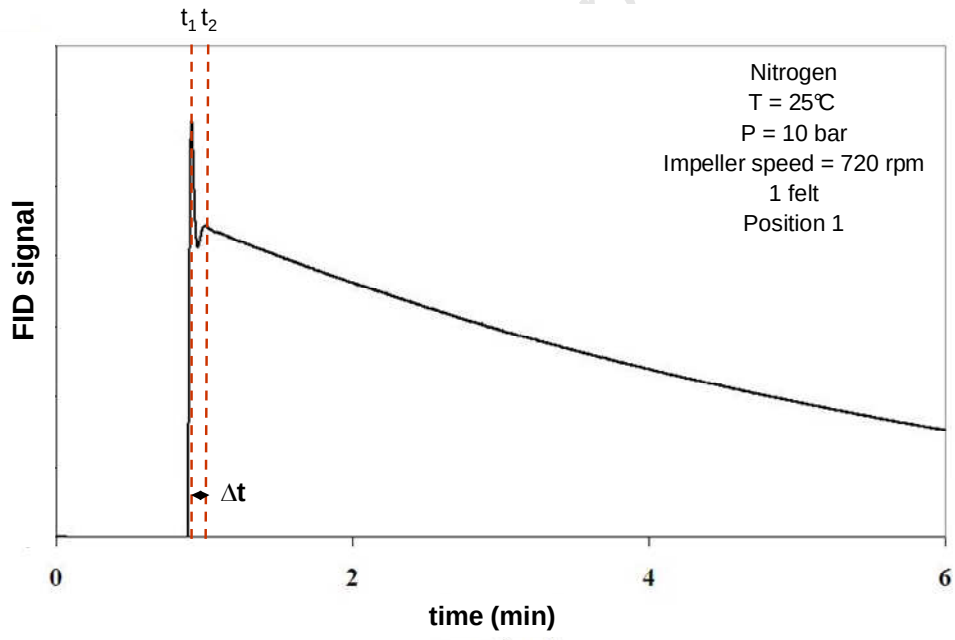

Figure 5.5: Typical tracer response in nitrogen feed gas with 1 felt in place

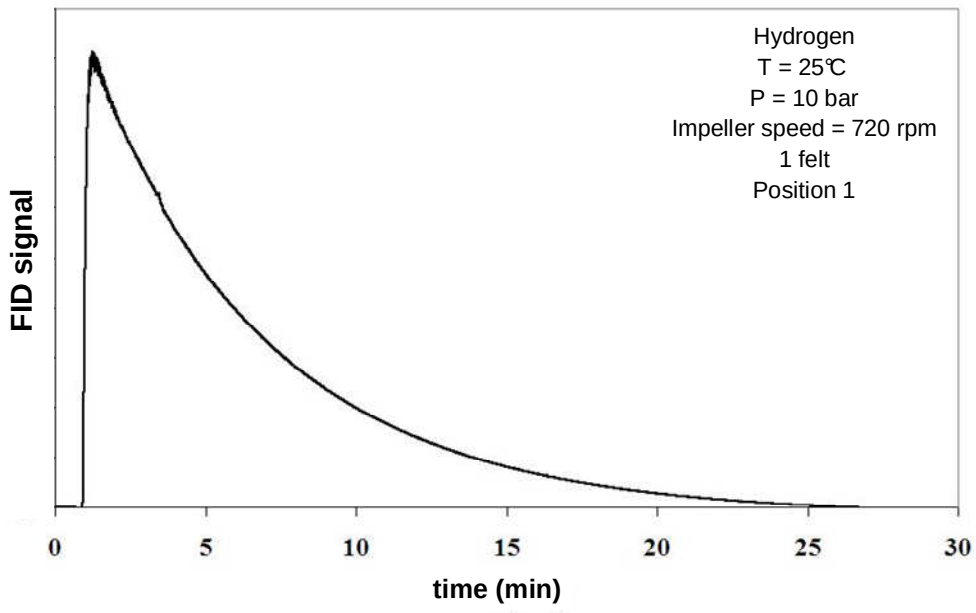

Figure 5.6: Typical tracer response in hydrogen feed gas with 1 felt in place

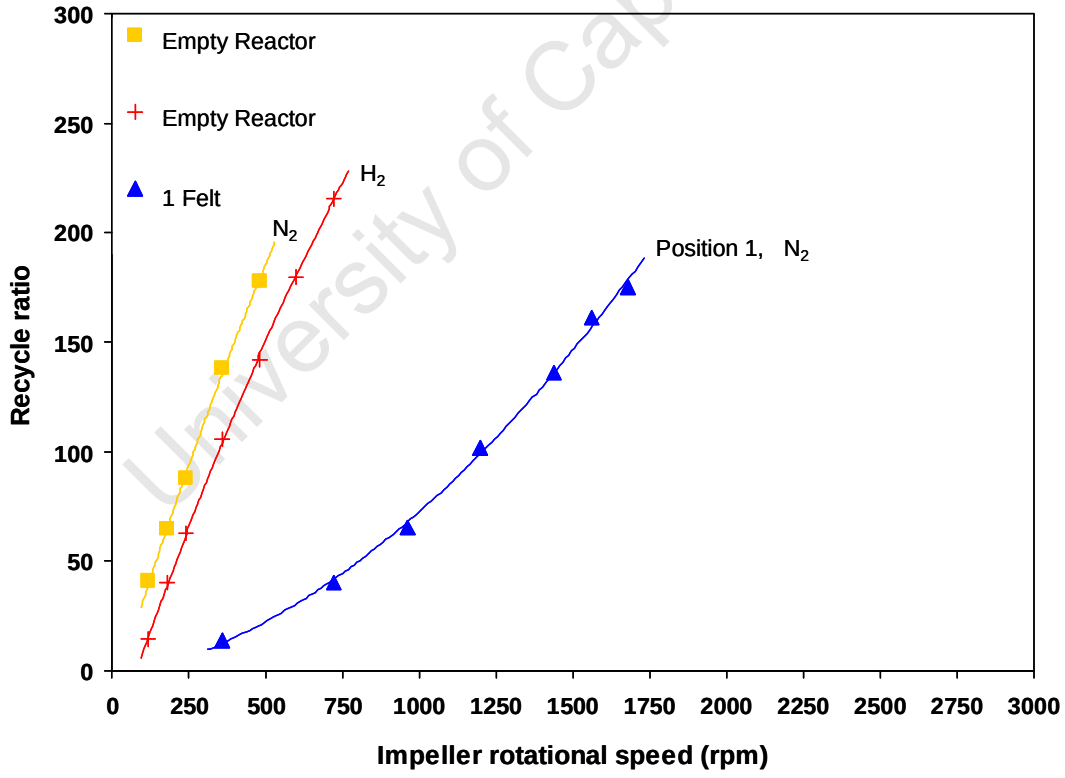

Figure 5.7: Comparison of recycle ratios obtained in empty reactor and reactor with one felt*

*__Note__: Quadric trend lines are used in the presentation of the experimental data once the felts are introduced. Refer to Appendix III for further discussion.

5.2.3 Two felts

The final set of experiments with regards to the addition of the internal components was carried out after inserting the second felt in the reactor. With both metal felts in place, a catalyst basket is formed with the top and bottom felt forming the ceiling and floor of the catalyst basket, respectively. A typical tracer response curve for each of the feed gases is presented in Figures 5.8 and 5.9, respectively. The effect of increasing impeller speeds on recycle ratios is presented in Figure 5.10.

As is shown in Figure 5.10, the recycle ratios obtained for nitrogen are further decreased with the additional increase in resistance to the gas flow offered by the additional felt. The absence of the second tracer peak in the hydrogen experiment (Figure 5.9) prevents a calculation of recycle ratios under these conditions.

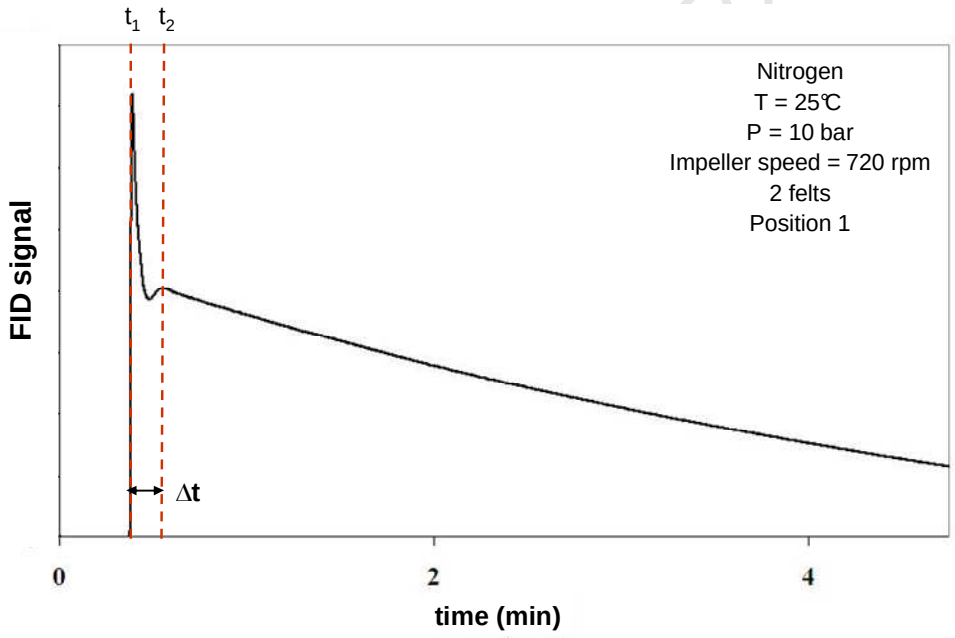

Figure 5.8: Typical tracer response in nitrogen feed gas with 2 felts in place

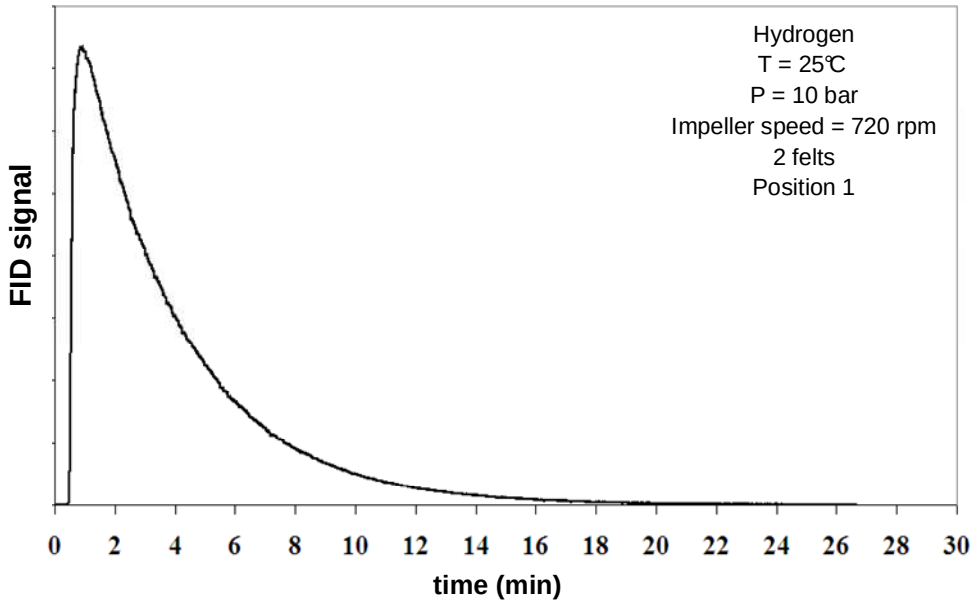

Figure 5.9: Typical tracer response in hydrogen feed gas with 2 felts in place

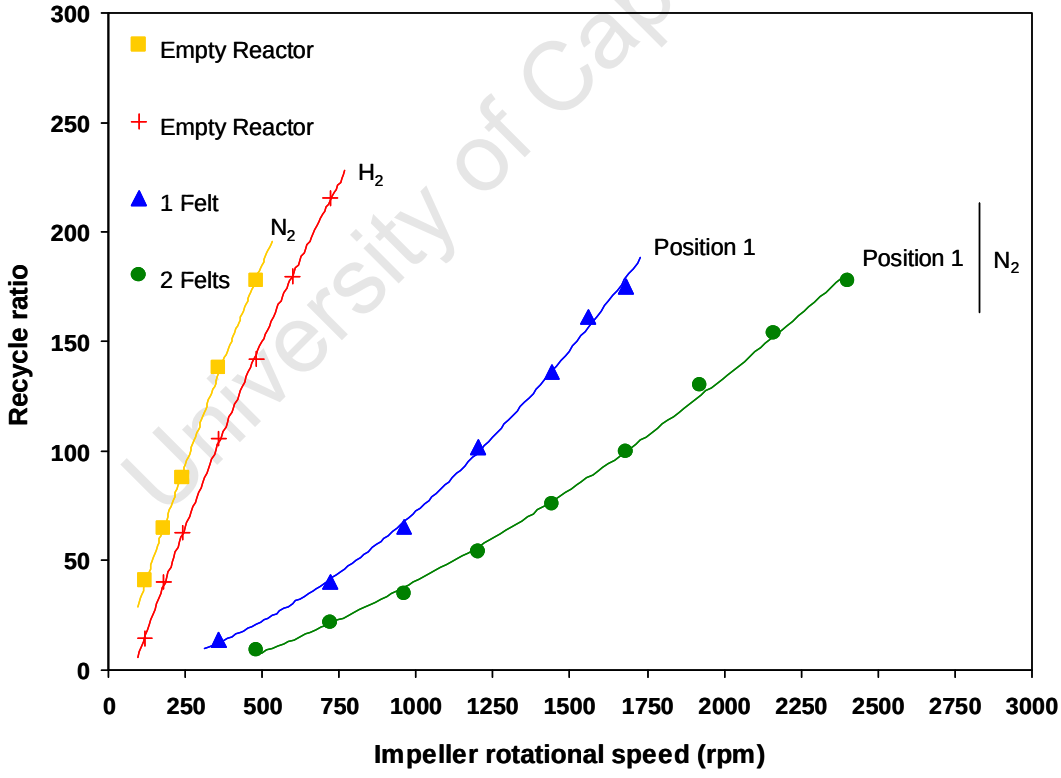

Figure 5.10: Comparison of recycle ratios obtained in empty reactor, reactor with one felt and reactor with two felts

5.2.4 Change in position of outlet capillary

In an attempt to clearly resolve the tracer recycle peaks in the hydrogen feed gas experiments and, hence, allow for determination of the recycle ratio, the positions of the inlet and outlet capillaries were changed to position 2 as indicated in Figure 5.1.

Experiments 3, 5 and 6 were repeated with the capillaries in position 2 (Experiments 7, 8 and 9, respectively). Figures 5.11 and 5.12 show the tracer response curves for both nitrogen and hydrogen as feed gases under the same conditions prevailing for experiments presented in Figures 5.8 and 5.9. As can be seen for the hydrogen feed gas experiment with the capillaries in position 2, the second tracer peak is now clearly visible, hence, enabling the calculation of recycle ratios in hydrogen with varying impeller speeds. This result, as well as that for nitrogen is shown in Figure 5.13.

Figure 5.13 clearly indicates the trends in recycle ratios with the change in various experimental parameters. The change in the position of the capillary enabled the visibility of the recycle peaks in the GC trace thus resulting in the recycle ratios for hydrogen to be calculated. With regards to nitrogen, there appears to be a discrepancy between the results obtained with the capillary in position 1 and 2, all other parameters kept constant.

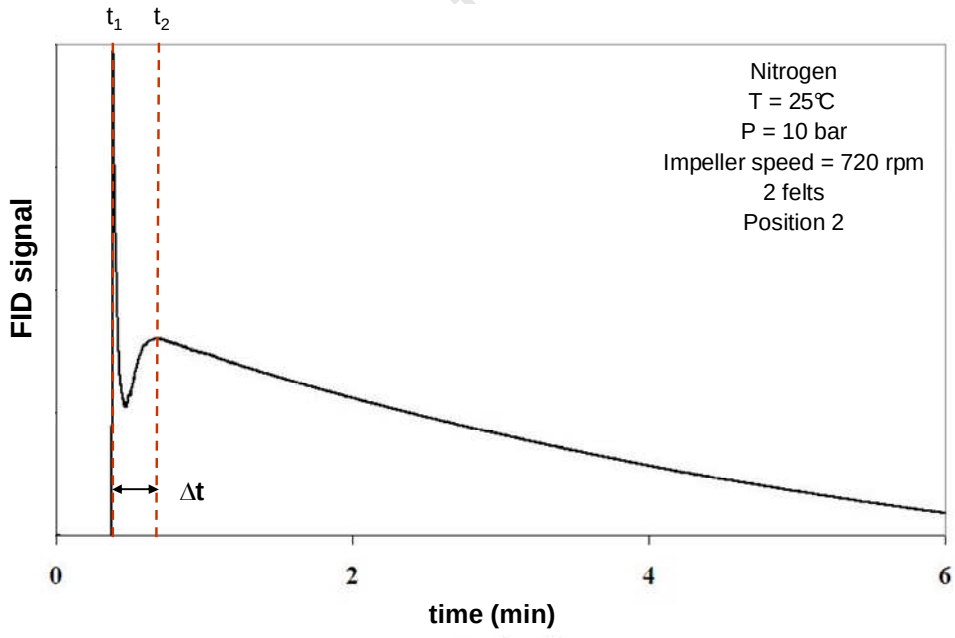

Figure 5.11: Typical tracer response in nitrogen feed gas with 2 felts in place and capillary in position 2

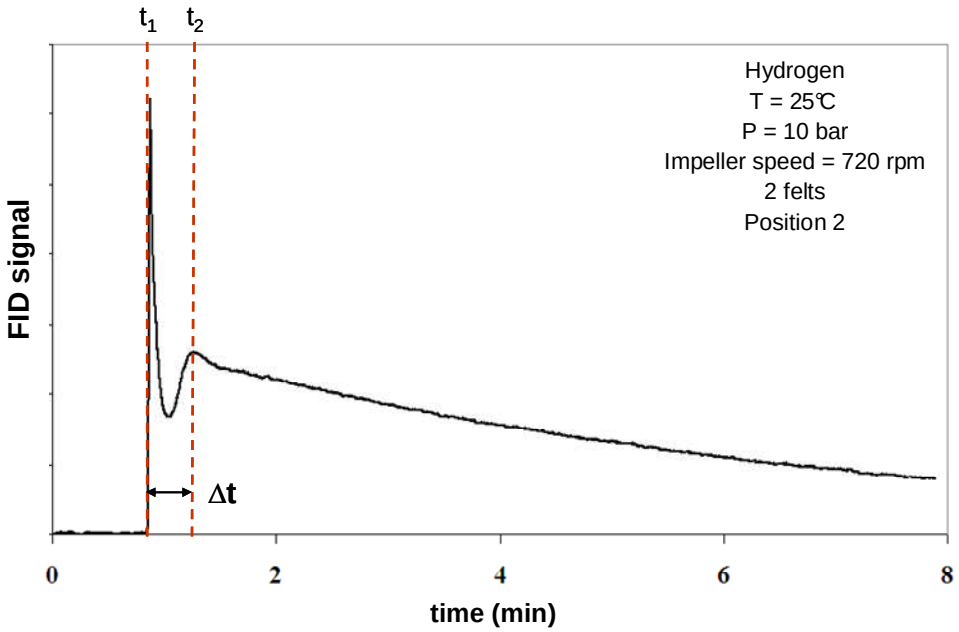

Figure 5.12: Typical tracer response in hydrogen feed gas with 2 felts in place and capillary in position 2

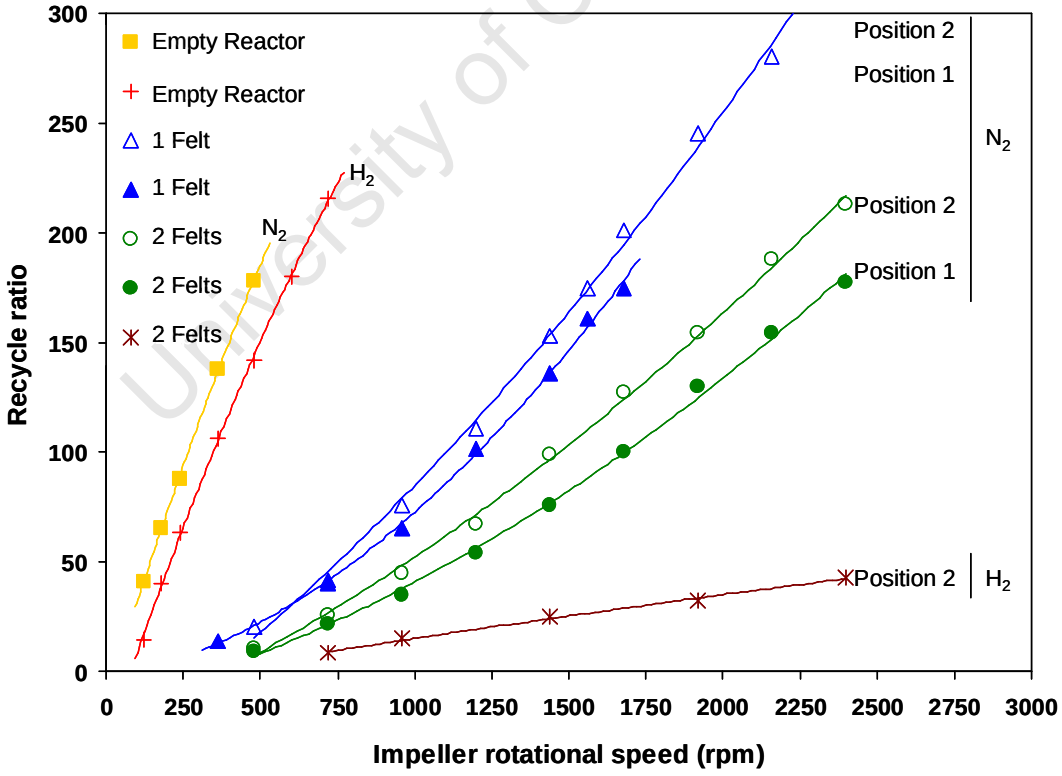

Figure 5.13: Comparison of recycle ratios obtained in empty reactor, reactor with one felt (Postion 1 and 2) and reactor with two felts (Postion 1 and 2)

5.2.5 Reproducibility of results

A reproducibility study was performed in order to ensure that the results presented are indeed a true reflection of the system. The reproducibility experiments were performed with two felts and 5 g of catalyst in place with the capillaries in position 2. Experiments were conducted at a temperature of 25℃ and 20 bar using nitrogen feed gas. The results from the experiment are presented in Figure 5.14.

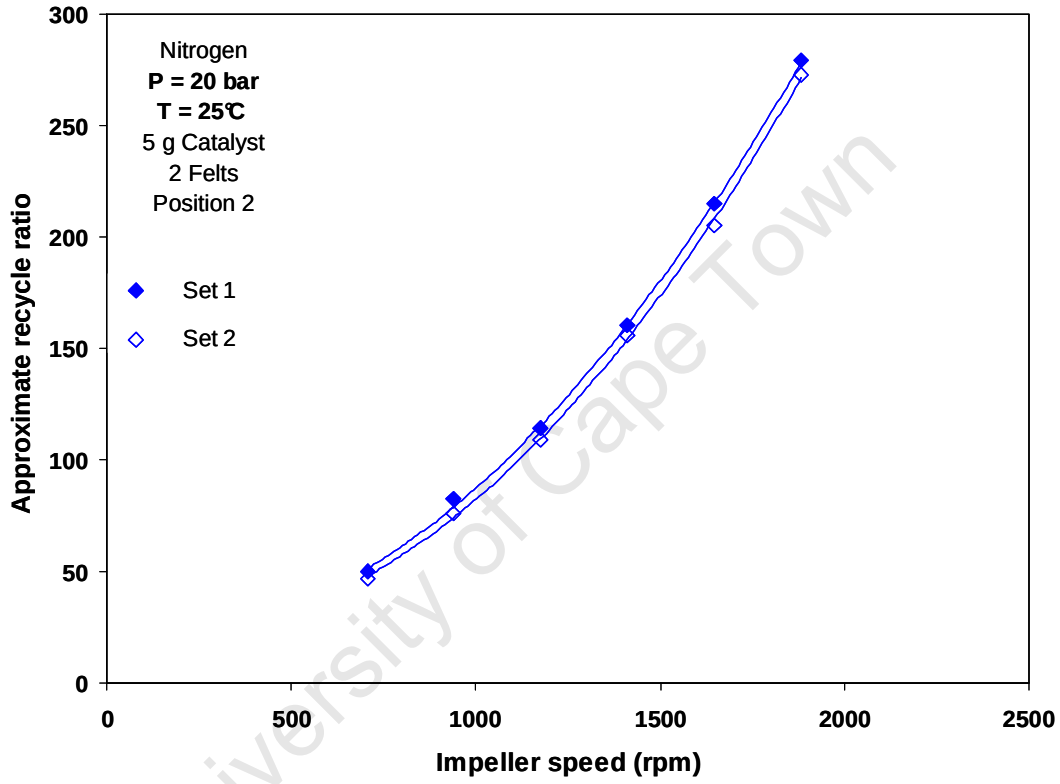

Figure 5.14: Results of reproducibility study

Experiment Set 1 and Set 2 were performed 4 weeks apart with a number of experiments being performed during this period. The scatter appears to be fairly uniform with the largest difference, of 8%, being observed at an impeller speed of 1600 rpm. From these results, is can be deduced the results are satisfactorily reproducible.

A second reproducibility study was performed at a temperature of 25℃ and pressure of 20 bar, with nitrogen feed gas. Once again, 5g of catalyst was used and two felts were in place with the capillaries in position 2. For this set of experiments, however, the impeller speed was kept constant at 1400 rpm. Ten experiments were performed under these exact conditions.

The standard deviation was then calculated to determine the accuracy of the result. The absolute recycle ratio obtained was **147 ± 2.65**. This once again confirms that the results obtained are sufficiently reproducible.

Overall, good reproducibility is observed. This confirms that the system is indeed operating satisfactorily and can be confidently used for the follow-on characterization experiments.

5.3 Discussion

5.3.1 Conventional RTD experiments – Capillary position 1

The results presented in Section 5.2.1 return the expected outcome of the recycle ratio increasing with increasing impeller speed. This is due to the fact that as the impeller is at greater angular velocities, gas internal to the reactor is circulated at a faster rate. Furthermore, the fact that nitrogen effects a greater recirculation (recycle ratio) than hydrogen can be attributed to the difference in densities of the two gases. Nitrogen, being the denser (higher molecular mass) of the gases effects a larger momentum transfer from the impeller thus resulting in increased recycle gas flow.

With regard to the range of measurability, above recycle ratios of approximately 200 (in this case above impeller speeds of 800 rpm), the tracer recycle peaks can no longer be clearly distinguished and hence recycle ratios can no longer be accurately determined. This phenomenon may be ascribed to the fact that at elevated stirrer speeds (and, hence, higher recycle flows), gas mixing internal to the reactor is increased to such an extent that dispersion of the methane tracer pulse into the feed gas is almost instantaneous and, hence, the tracer peaks can longer be detected.

The introduction of the felts into the path of the gas stream passing through the catalyst basket generates a pressure drop due to the resistance offered by the metal felts. The felts clearly present a substantial flow resistance as may be observed in the results of experiments with nitrogen feed gas, as is presented in Figure 5.7, where a substantial decrease in recycle ratio is seen with the introduction of the metal felt.

For hydrogen, the increased flow disturbance offered by the felt is enough to sufficiently disperse the second methane tracer peak to the point where it can no longer be detected (Figures 5.5 and 5.6). At first inspection, the CSTR like resemblance of the tracer response suggests that the mixing is almost perfect. However, from previous results (Figure 5.4) it was already shown that the recycle flow is higher with nitrogen and, hence, the recycle ratios effected with hydrogen should be lower. The disappearance of the tracer recycle peaks in the case of hydrogen feed gas is presumably due to a faster dispersion of methane in hydrogen as compared to nitrogen. Moreover, the resistance offered by the felt decreases the recycle gas flow rate which in turn increases the time for the dispersion of the tracer pulse between detection periods. The methane tracer pulse is dispersed too rapidly in hydrogen and thus cannot be detected by the GC. The same occurs in the case of nitrogen but not to the extent where the pulse can no longer be detected.

With a second felt in place, the additional flow resistance serves to exacerbate the effects observed with the introduction of the first metal felt. The recycle ratios obtained for nitrogen are further decreased and once again, those for hydrogen are incalculable due to the inability to observe the tracer recycle pulses. This result is expected since the addition of a second felt increases the flow resistance and, hence, reduces the recycle flow whilst compounding the problem of the tracer dispersion. In order to measure the methane pulse and, hence, calculate the recycle ratios under these conditions, an alternative tracer detection methodology is required.

5.3.2 Modified RTD experiments – Capillary position 2

With the conventional configuration of placing the inlet and outlet capillaries at the reactor inlet and outlet respectively (Figure 5.15a), it is necessary that the methane tracer pulse makes almost a complete recycle before the first peak is detected (Figure 5.15b). Keeping in mind that a minimum of two peaks need to be detected in order to calculate the recycle ratio, the tracer pulse is required to make another second complete recycle, along the path shown in Figure 5.15c, before the second tracer peak is detected. It is during this time period (for the tracer to circulate twice around the internal recycle loop) that the tracer pulse is dispersed, both by diffusion and convective turbulence, to an extent in the case of hydrogen that the second (recycle) pulse is no longer detectable.

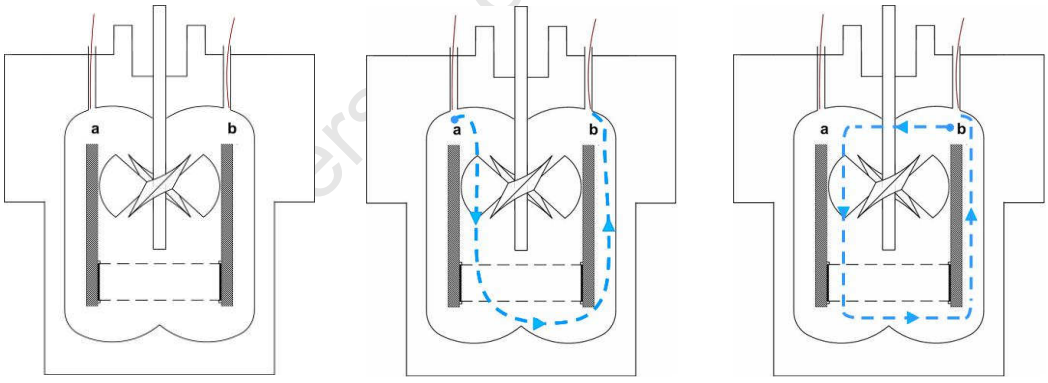

Figure 5.15: Path of recycle loop (a) Capillary in position 1, (b) Flow of gas before first peak is detected (c) Complete recycle loop before second peak is detected

In order to minimise the time allowed for dispersion of the methane pulse into the feed gas, the outlet capillary was inserted through the catalyst bed (from bottom up) and the inlet capillary placed just above the catalyst basket as shown in Figure 5.16a. In this configuration, the first tracer peak can now be detected almost immediately after tracer injection and the second after a single complete recycle (Figures 5.16b and 5.16c) thus effectively halving the

time (and length of the tracer dispersion path) required for the detection of the first two tracer recycle pulses needed for the determination of the recycle ratio.

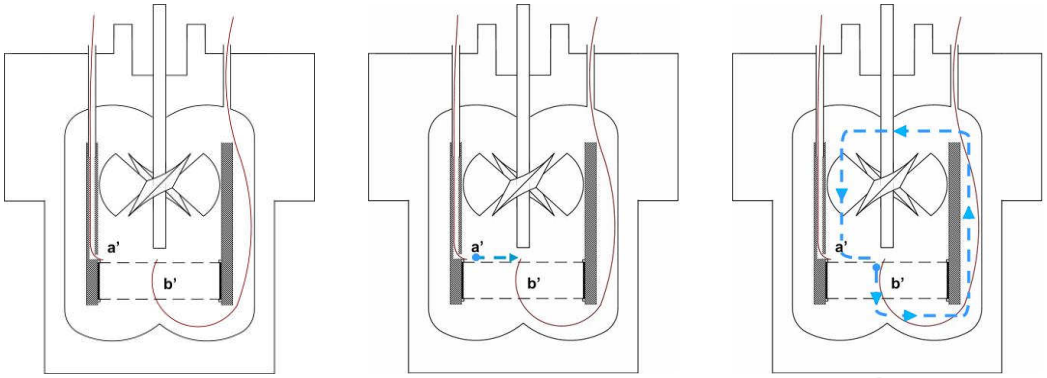

(a) (b) (c)

Figure 5.16: Path of recycle loop (a) Capillary in position 2, (b) Flow of gas before first peak is detected (c) Complete recycle loop before second peak is detected

From the results presented in Section 5.2.4, the effect of the change in capillary position can clearly be seen. The previously undetectable tracer recycle pulses in hydrogen feed gas are now readily resolved (Figure 5.9) allowing for accurate determination of the recycle ratios as presented in Figure 5.10. As expected the recycle ratios obtained for hydrogen are substantially lower than those obtained with nitrogen as the feed gas and, additionally, it can be seen that the resistance offered by the second metal felt further reduces the effective recycle ratio.

An interesting observation, however, is the difference in recycle ratios determined for capillaries placed in position 1 versus position 2, while keeping all other conditions unchanged. This difference is observed in the case of experiments having both a single and two felts in the recycle flow path (Figure 5.10) where it appears that recycle ratios measured using capillaries in position 2 are consistently and proportionately higher than when measured using capillaries in position 1 (the conventional inlet and outlet position for RTD studies). This can be attributed to the fact that in position 2, there is still a 3 cm horizontal distance between the inlet and outlet capillaries, with the former being at the periphery of the central flow path and the latter right in the centre thereof. In part, this arrangement is to avoid a concentrated input signal from saturating the detector electronics were the position 2 inlet capillary being co-incident with that of the outlet capillary.

A consequence, however, of this arrangement is that by the time the inlet tracer pulse has reached the central outlet capillary (via diffusion), downwards convective flow has driven the main tracer input some distance along the principle recycle path, i.e. the initial detection of the

tracer is from a point in the tracer distribution tail at a time when the tracer distribution peak has already traversed some distance along the recycle path. By the time the tracer pulse returns to the central outlet capillary position – and the second 'recycle' pulse is detected – the tracer is uniformly spread across the internal diameter of the draft tube flow path. The same is true for any subsequent recycle tracer pulses which may be detected, i.e. third or fourth tracer pulses if indeed these are still measurable. Thus the first recycle period (the period between the first two tracer pulses detected) is systematically shorter than the second subsequent recycle period resulting in an overestimation of the recycle ratios when using the first two tracer pulses only. This error may thus be classified as systematic error which, from Figure 5.10 appears to be of the order of a 25% overestimation throughout the stirrer speed range.

That this explanation is correct is confirmed for those cases where three recycle tracer peaks are detected. In such cases it is observed that the peak-to-peak period between the first and second tracer pulse is shorter than the peak-to-peak interval between the second and third tracer pulses. This is due to the methane tracer pulse completing a full recycle path between detection of the second and third tracer pulses. The recycle ratio obtained using the second to third peak interval is in agreement (within reasonable error) with those results obtained under the same conditions for capillaries in position 1. However, under most conditions, the third peak (after a second recycle) cannot be discerned in the tracer responses and hence the peak-to-peak interval between the first and second tracer pulses needs to be used for estimation of the recycle ratios. Consequently, in the case of findings in Chapter 6, where recycle ratios have been determined with capillaries in position 2, these should be considered as an overestimation by approximately 25%.

Although the use of capillaries in position 2 results in an overestimation of the recycle ratios (by roughly 25%), the method offers two distinct advantages over the conventional RTD inlet and outlet positions (capillary position 1), viz.

i. A reasonable estimate of the recycle ratio can be obtained under conditions for which the conventional approach yields no results at all, and

ii. A direct confirmation that the generally mixed flow result determined from the RTD response is, indeed, due at least in part from adequate recycle flow through the catalyst bed and not merely a consequence of other fluid phase mixing phenomena (e.g. impeller mixing) which are not indicative of adequate fluid catalyst contact and true CSTR behaviour.

6. Residence time distribution study – Reactor characterization

6.1 Experimental

Characterization of the reactor was undertaken by means of a residence time distribution study to determine the effect of various parameters on the recycle flow in the reactor. The general method described in Section 2.4.2 was applied as per the specific experimental procedure developed in Section 5 with inlet and outlet capillaries in position 2. Table 6.1 lists all experiments conducted in the reactor characterization study. A fold-out of the experimental lists can be found in Appendix II.

Table 6.1: List of experiments performed in method development study

	Gas	Pressure	Temperature	Catalyst Mass
Exp 10	HYDROGEN	10 bar	25℃	5 g
Exp 11			100℃	
Exp 12			200℃	
Exp 13			300℃	
Exp 14		20 bar	25℃	
Exp 15			100℃	
Exp 16			200℃	
Exp 17			300℃	
Exp 18		30 bar	25℃	
Exp 19			100℃	
Exp 20			200℃	
Exp 21			300℃	
Exp 22	NITROGEN	10 bar	25℃	
Exp 23			100℃	
Exp 24			200℃	
Exp 25			300℃	
Exp 26		20 bar	25℃	
Exp 27			100℃	
Exp 28			200℃	
Exp 29			300℃	
Exp 30		30 bar	25℃	
Exp 31			100℃	
Exp 32			200℃	
Exp 33*	SYNGAS	20 bar	25℃	
Exp 34	NITROGEN	10 bar	25℃	0 g
Exp 35				10 g
Exp 36		20 bar		10 g

* Impeller speed constant at 720 rpm, composition of syngas varied

All experiments were performed with a feed gas flowrate of 1500 sccm, 2 felts in place and with inlet and outlet capillaries in position 2. The impeller speed was varied from 720 rpm – 2000 rpm, unless otherwise indicated.

Please refer to Appendix II for a fold-out of the experimental lists.

6.2 Results

The results from Experiments 22-32 are presented in two sets of figures. The first showing the effect of pressure (Figures 6.2 – 6.5, Section 6.2.1) and the second showing the effect of temperature (Figures 6.6 – 6.8, Section 6.2.2). Both sets of results are presented showing the effect of change in recycle ratio with increasing impeller speed under various combinations of temperature and pressure.

6.2.1 Effect of pressure

For the experiments using hydrogen as the feed gas, results were obtained at 25℃ (Exp 10, 14 and 18) (Figure 6.1). For temperatures greater than 25℃ (Exp 11-13, 15-17 and 19-21), the tracer response peaks were not adequately distinguishable to allow for the calculation of the prevailing recycle ratios. All subsequent experiments were thus performed using nitrogen as the feed gas.

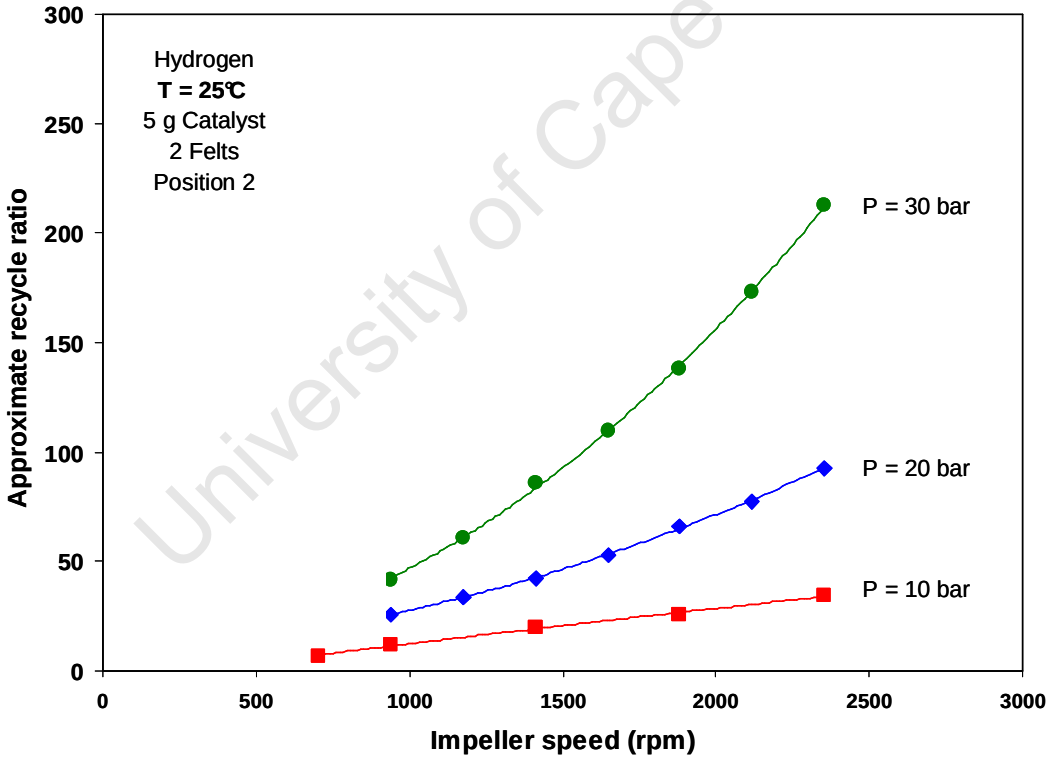

Figure 6.1: Recycle ratio as a function of impeller speed and pressure – Hydrogen at T = 25℃

When comparing the results from Figures 6.1 and 6.2, it can be seen that the results from these experiments are in agreement with the findings of the method development study where the recycle ratios calculated for hydrogen are significantly lower than those obtained with nitrogen.

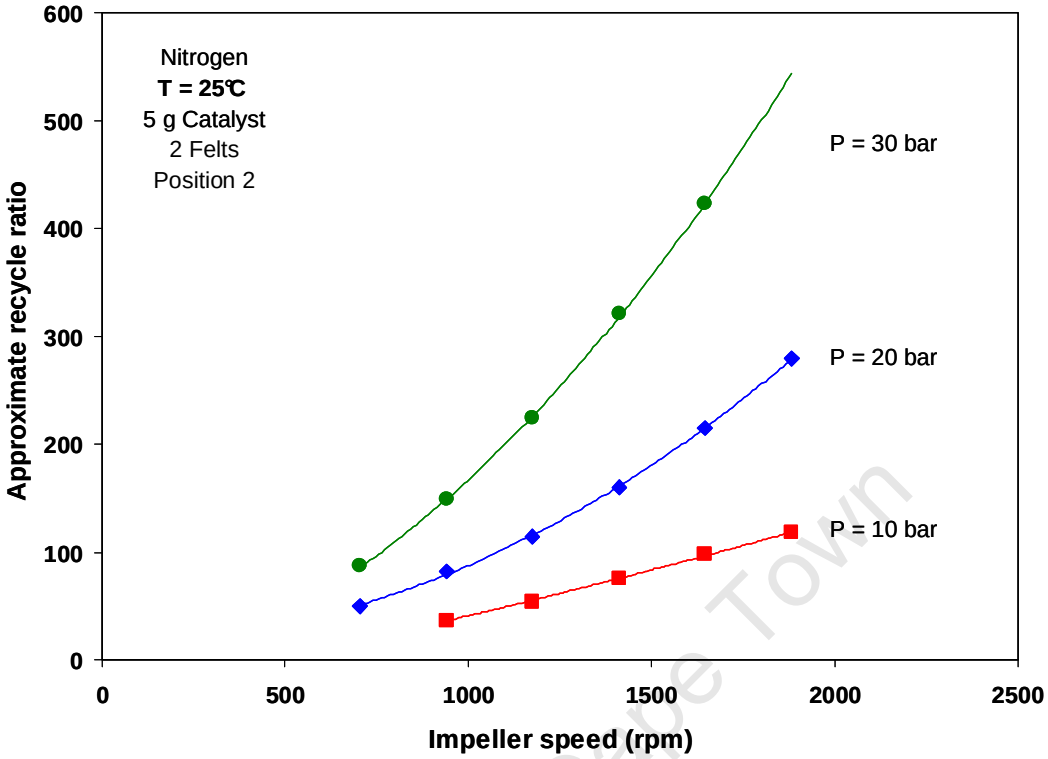

Figure 6.2: Recycle ratio as a function of impeller speed and pressure – Nitrogen at T = 25℃

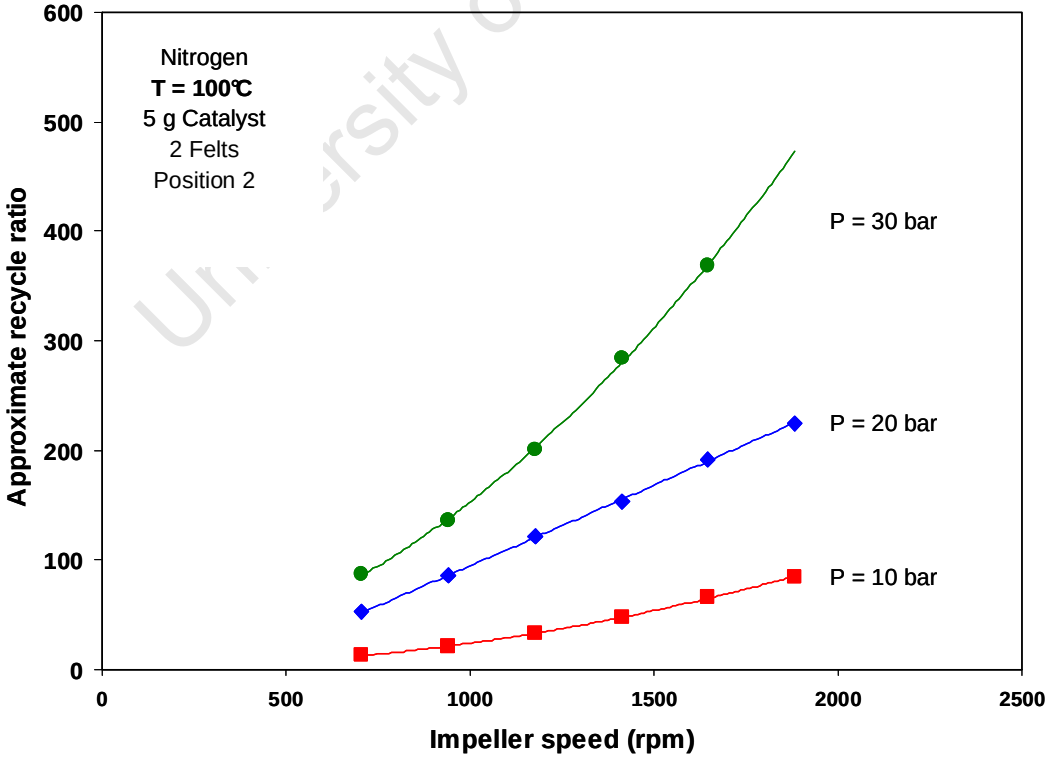

Figure 6.3: Recycle ratio as a function of impeller speed and pressure – Nitrogen at T = 100℃

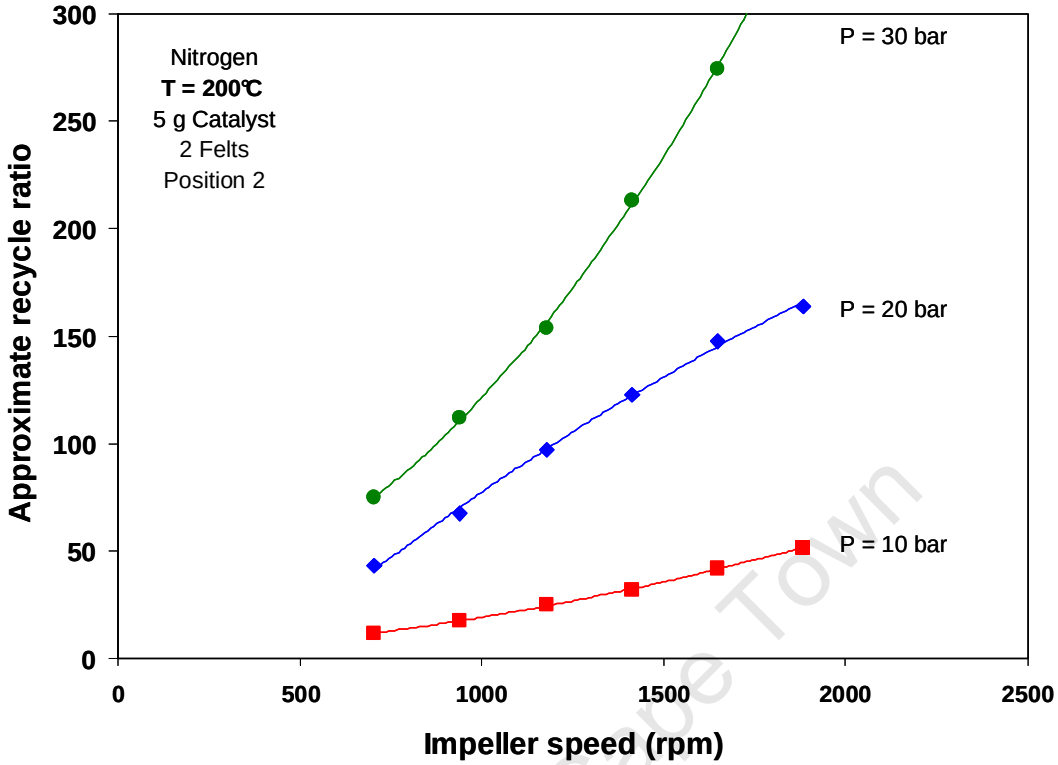

Figure 6.4: Recycle ratio as a function of impeller speed and pressure – Nitrogen at T = 200℃

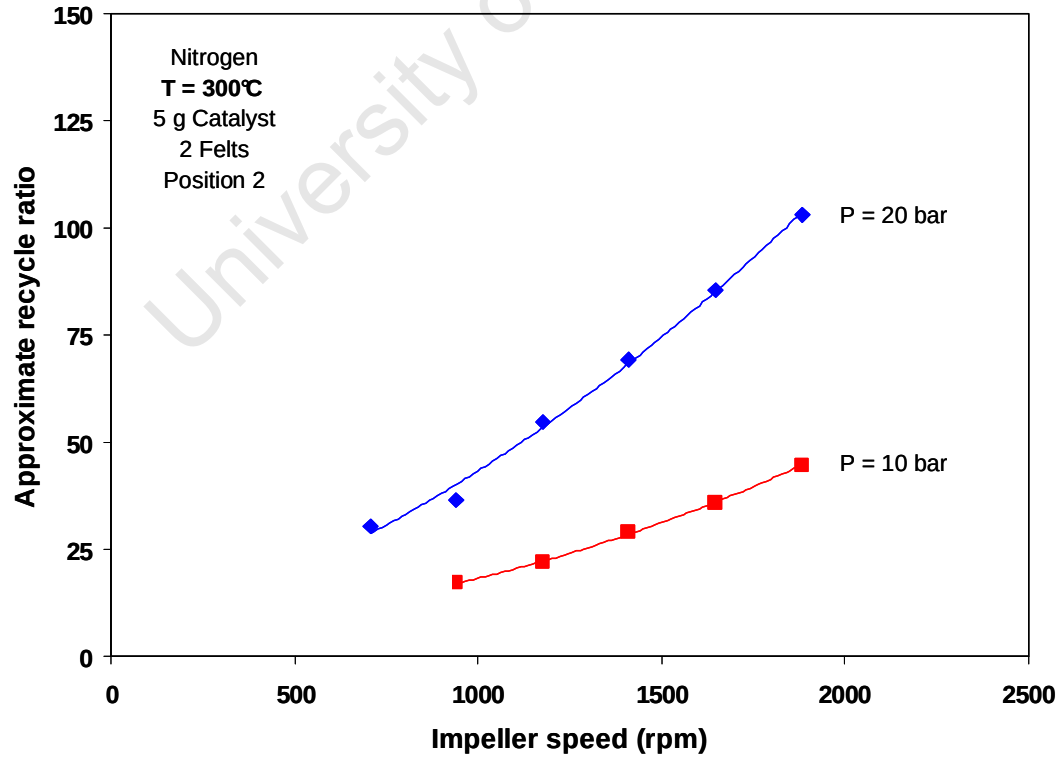

Figure 6.5: Recycle ratio as a function of impeller speed and pressure – Nitrogen at T = 300℃

From Figures 6.2 – 6.5 it is evident that the recycle ratio increases with increasing pressure. It can be seen that the absolute difference becomes more pronounced at higher impeller speeds. At pressures of 20 bar and above, recycle ratios substantially greater that 20 are achieved, even at low impeller speeds.

6.2.2 Effect of temperature

The second set of figures show the same results as per Section 6.2.1, however, here they are presented, for different pressures, showing the effect of temperature on the recycle ratios at varying impeller speeds.

It can be seen from Figures 6.6 – 6.8 that the recycle ratio decreases with an increase in temperature. Furthermore, as the temperature increases the absolute difference becomes smaller.

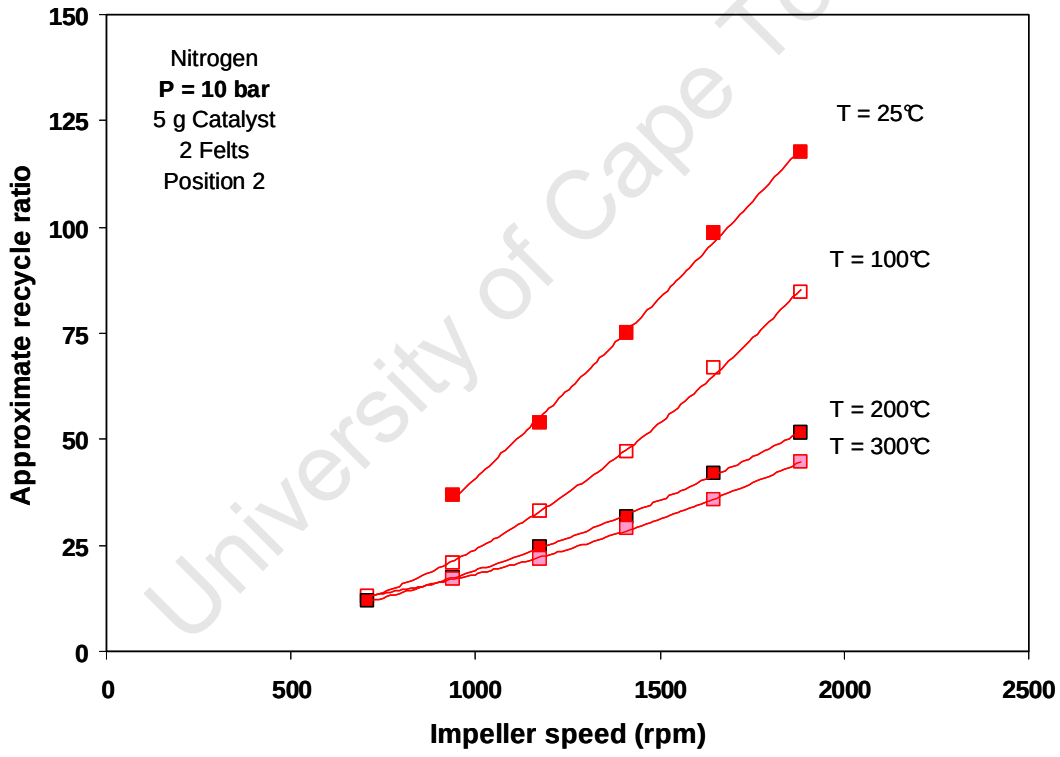

Figure 6.6: Recycle ratio as a function of impeller speed and temperature – Nitrogen at P = 10 bar

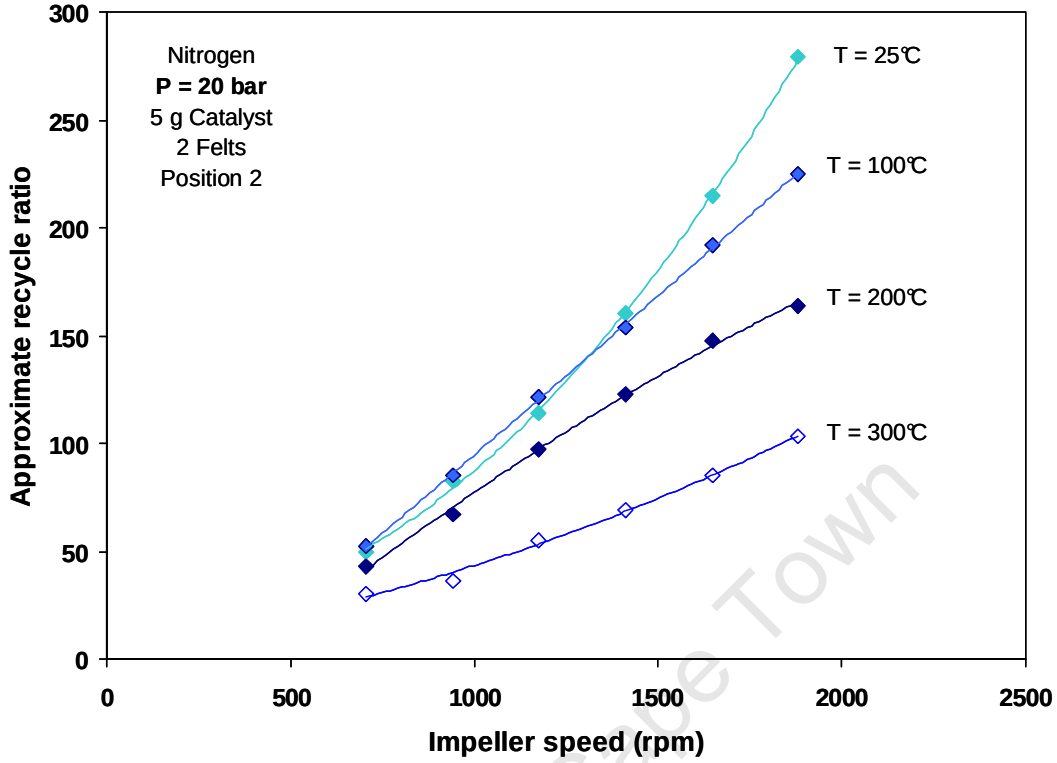

Figure 6.7: Recycle ratio as a function of impeller speed and temperature – Nitrogen at P = 20 bar

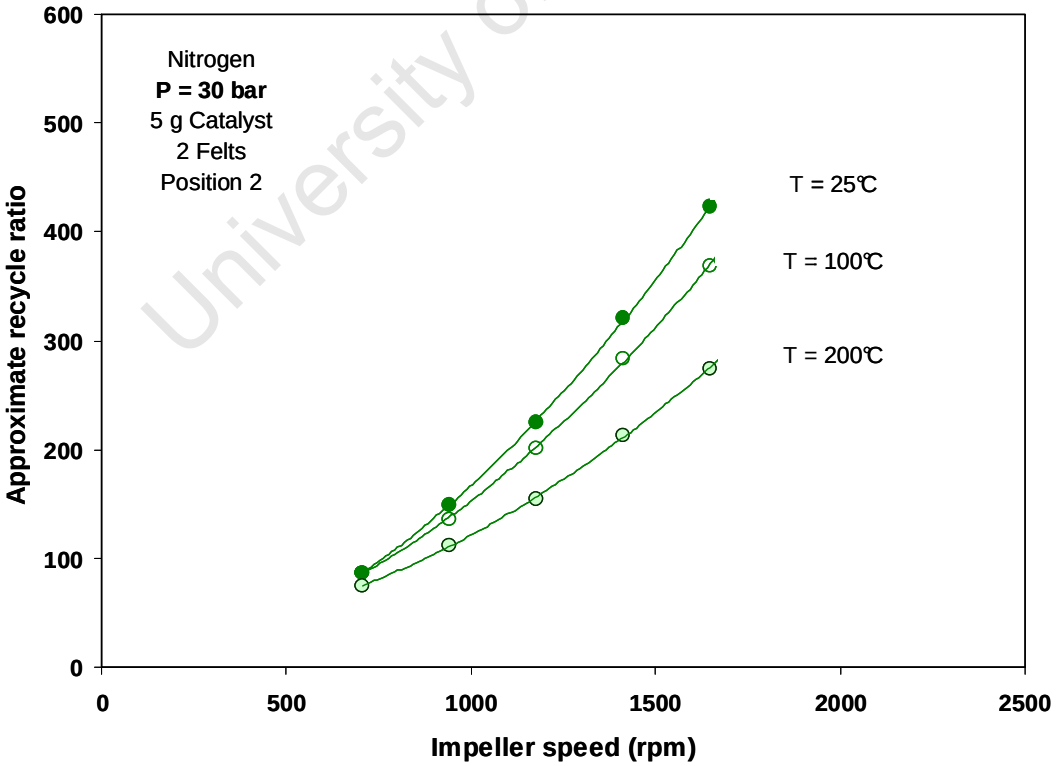

Figure 6.8: Recycle ratio as a function of impeller speed and temperature – Nitrogen at P = 30 bar

6.2.3 Effect of catalyst mass

The effect of catalyst mass on the recycle ratios is presented in Figure 6.9 at pressures of 10 and 20 bar; with no catalyst (only at 10 bar), 5 g of catalyst and 10 g of catalyst.

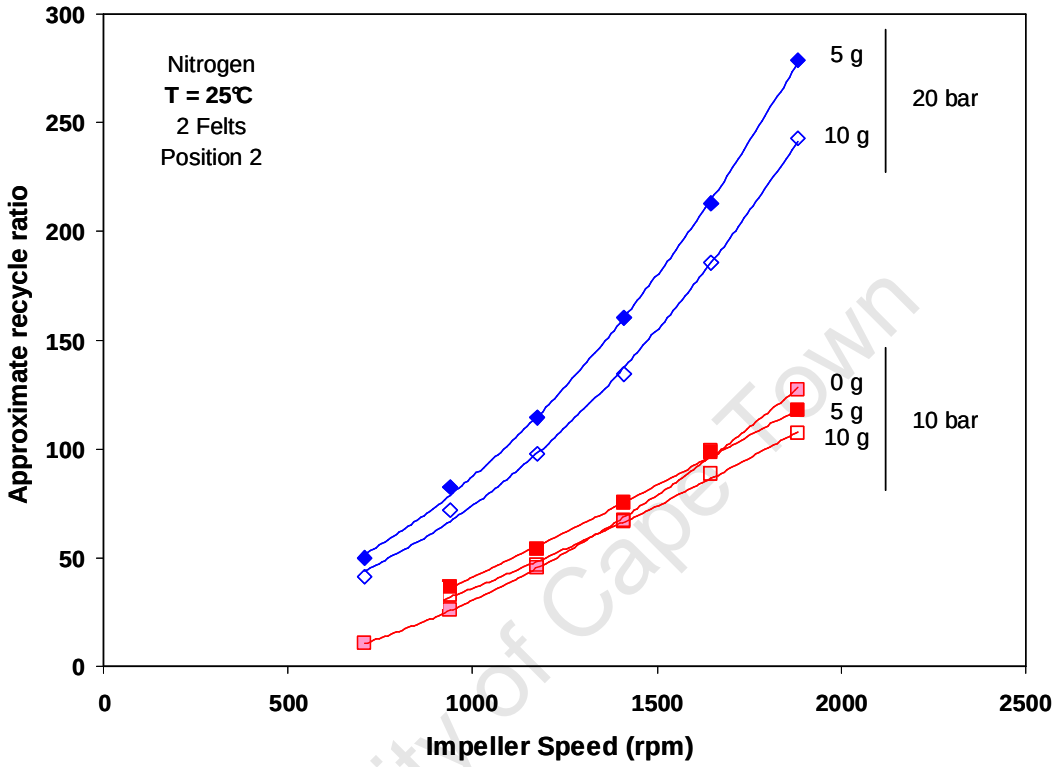

Figure 6.9: Effect of catalyst mass on recycle ratios

The amount of catalyst placed in the catalyst basket does not have much effect on the recycle ratio (Figure 6.9), although the effect is slightly more pronounced at higher pressures. Clearly the principal flow restriction is that provided by the felts.

6.2.4 Effect of syngas composition

Keeping in mind that the STIRR is aimed for use in Fischer-Tropsch catalyst testing, the recycle ratio was measured for various syngas compositions (carbon monoxide and hydrogen in various ratios). The results are presented in Figure 6.10.

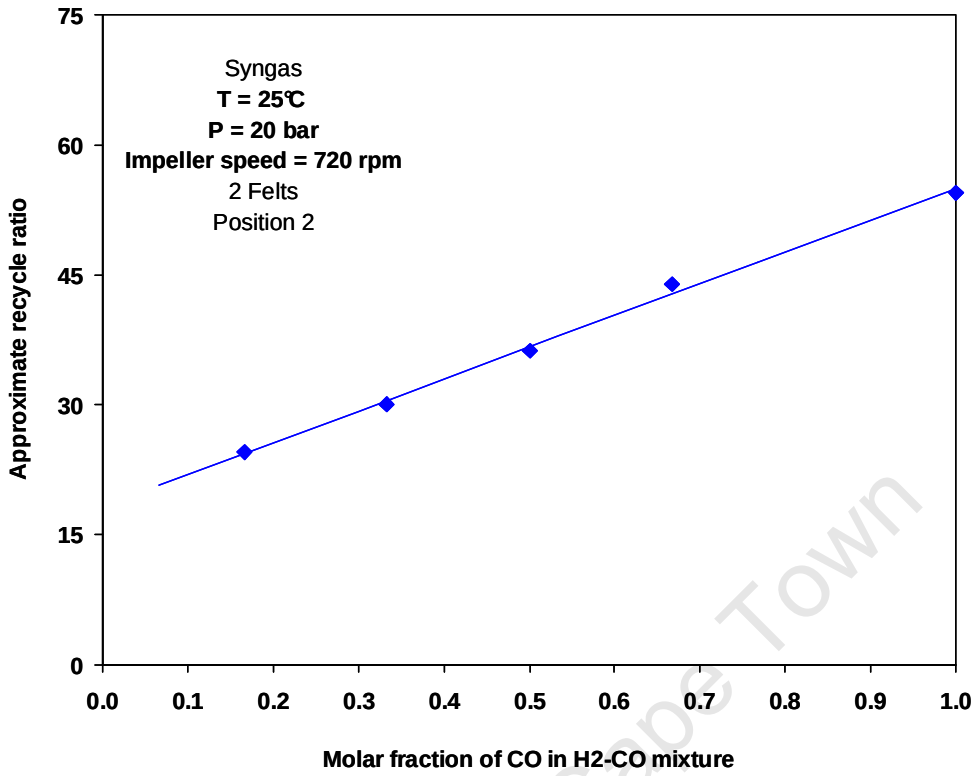

Figure 6.10: Effect of syngas composition on recycle ratios

Figure 6.10 clearly indicates that the recycle ratio increases with decreasing molar fraction of hydrogen consistent with the effect of gas density in the hydrogen versus nitrogen experiments shown in the method development study (Section 5). At a mole fraction of H_2/CO of 2, ubiquitous to Fischer-Tropsch synthesis, the recycle ratio is approximately 35 at a temperature of 25℃ and 20 bar, at an impeller speed of 720rpm.

6.2.5 Recycle flow under HTFT conditions

The final experiment was performed at HTFT conditions (300℃ and 20 bar) at a fixed impeller speed of 960 rpm with nitrogen feed gas. An initial attempt to perform this experiment using a syngas feed failed due to product forming under the HTFT conditions employed. As a result the methane tracer peaks could no longer be clearly distinguished, preventing the determination of the recycle ratio. Consequently, it was decided to use nitrogen feed gas to conduct the experiment.

Under these conditions a recycle ratio of **37** was obtained.

6.3 Discussion

6.3.1 Effect of pressure, feed gas and temperature

From the results presented in Figures 6.1 – 6.6, two observations can be made. The first being that the recycle ratio increases with an increase in pressure, whilst feed gas mass flow rate is kept constant. The feed gas mass flow rate is the same in all experiments in this study and reflects standard operating FT synthesis conditions. A given feed gas mass flow rate delivered at higher pressure gives a proportionally lower volumetric flow rate and by consequence higher residence time.

It can therefore be said that the recycle ratio increases with increasing residence time. The findings from similar experiments performed with a jetloop reactor appear to be counter intuitive as they demonstrate that in that particular reactor the recycle ratio is inversely proportional to the residence time (Möller 1995).

In a jetloop reactor the pressure drop over the inlet jet is a result of the feed gas flow rate through the jet which is set by a mass flow controller upstream of the jet (See Section 2.2.2). At high feed flow rates the mean residence time will be low. A high feed flow rate that is being forced through the inlet jet requires a higher pressure on the upstream side than a small feed flow rate. Thus the pressure drop over the inlet jet is high upon setting a high feed flow rate. Pressure equals force per unit of cross sectional surface area. The force associated with the changing momentum of a fluid is equal to the rate of mass flow times its change in velocity. The former is set and the latter simply follows from the dimensions of the inlet jet and the set pressure in the jetloop reactor. The power of the jet which is the rate of energy delivered to the reactor equals the force times the velocity of the jet. Therefore a higher pressure drop in the inlet jet due to a higher flow rate through the inlet jet gives a higher energy input to overcome the pressure drop of the recycle loop which contains the catalyst bed. Assuming then that at constant pressure in the jetloop reactor the mean residence time is varied by increasing the feed mass flow rate through the inlet jet, the higher pressure drop over the inlet jet propels the gas along the internal recycle loop and gives rise to a higher recycle ratio at shorter residence times.

In a STIRR a device external to the reactor, the impeller, not the inlet gas stream, drives the gas through the internal recycle loop. In this case the rate of energy input is the power delivered by the impeller to the fluid and this power is independent of the flow rate of the feed gas and thus it is independent of the residence time of the gas in the STIRR.

The second observation that can be made is that, where data could be obtained from the experiments using hydrogen feed gas, the recycle ratios obtained with nitrogen are greater than those obtained with hydrogen (as briefly discussed in Section 6.2.1). This phenomenon was attributed to nitrogen being the denser of the two gases, hence experiencing a larger momentum transfer from the impeller onto the internal gas and, consequently, resulting in increased recycle flow. During these experiments, the reactor was empty (no felts in place offering resistance to flow) and, hence, the dominant factor affecting the recycle flow is the gas density (molecular mass) with drag resistance along the internal recycle path being negligibly affected by the other gas properties.

In order to interpret the influence of the catalyst basket (including felts, metal sieve plates and catalyst), one needs to consider the factors that drive the gas through the resistance offered by the catalyst bed. For this, the discussion presented in Section 2.3 pertains. The pressure head generated by the impeller drives the gas through the catalyst bed which offers resistance to flow. The pressure head developed for each of the gases, nitrogen and hydrogen, can be calculated using the tangential and axial components of the work done (see Figure 2.8). If one assumes that the gas molecules suffer only elastic collisions, then it follows their kinetic energy is conserved. The angular velocities at which the STIRR impeller is operated are roughly two orders of magnitude higher than the downflow recycle gas velocity. As a result, the relative velocity at which the gas approaches the impeller is almost at a right angle to the axial flow direction. Since the impeller blades are pitched at 45° to the axial dir ection, gas molecules impinging upon the impeller leave with an absolute velocity directed at approximately 45° to the vertical axis. The tangential component of the gas velocity, therefore, is almost exactly the same as the axial component. Consequently the energy transferred to the gas (as work done on the gas) is consumed to increase the enthalpy of the gas – which raises the static pressure – and the kinetic energy of the gas – which can be understood as dynamic pressure – in almost equal parts. The pressure drop across the catalyst bed for nitrogen and hydrogen at 25℃, 10 bar and an impeller speed of 1920 rpm was calculated to be 270 Pa and 20 Pa respectively (See Appendix IV for calculation). This clearly indicates that a substantially larger pressure drop is generated for nitrogen, as expected since nitrogen is the heavier of the two gases.

In addition to the influence of the pressure drop over the catalyst bed resulting in different extents of total flow (and, hence, recycle flow and recycle ratio) for each of the gases, as explained in Section 2.3.2, the influence of gas viscosity also plays a role. According to Equation 2.13,

$$\frac{\Delta p}{L} = au + bpu^2 \qquad \text{(Equation 2.13)}$$

$$\text{with } a = \frac{\mu}{B_0}$$

a good linear correlation between the pressure drop and the gas velocity demonstrates that viscous resistance dominates over inertial resistance, as is confirmed experimentally in Figure 6.11.

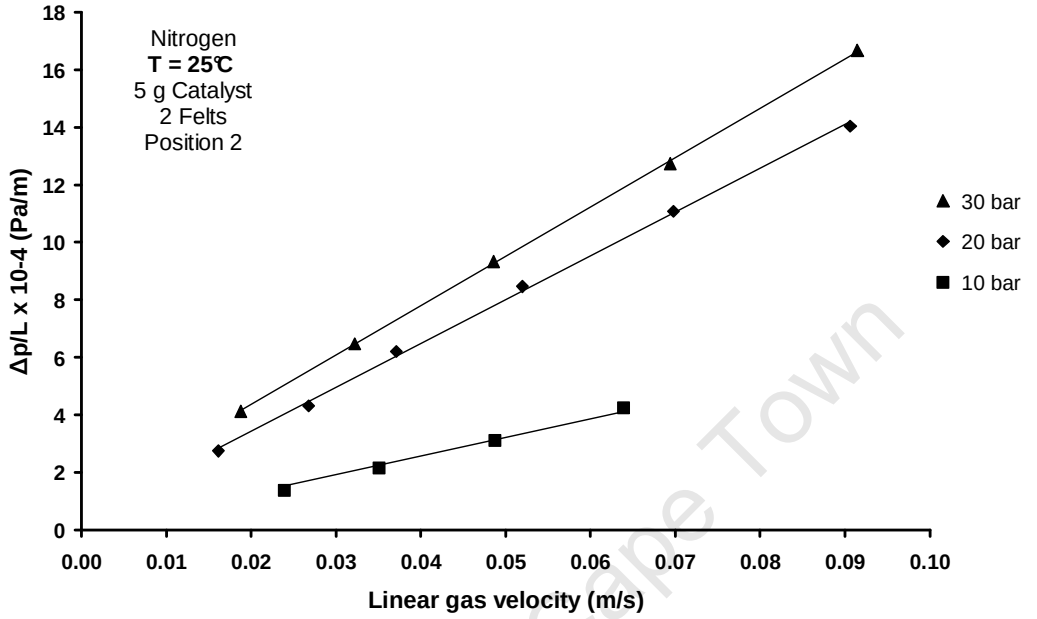

Figure 6.11: Plot of pressure drop versus gas velocity (Nitrogen, T = 25℃)

The viscosity of hydrogen and nitrogen gas at different temperatures, is presented in Table 6.2 from which it can be seen that the viscosity of nitrogen is approximately 2.5 times larger than that of hydrogen.

Table 6.2: Variation of the viscosity (μ) of hydrogen and nitrogen with temperature (Perry, 1973)

Temperature (℃)	25	100	200	300
$\mu(H_2)$ (kg/sm)	$7{,}2 \times 10^{-06}$	$8{,}4 \times 10^{-06}$	$9{,}8 \times 10^{-06}$	$11{,}1 \times 10^{-06}$
$\mu(N_2)$ (kg/sm)	$17{,}2 \times 10^{-06}$	$20{,}4 \times 10^{-06}$	$24{,}1 \times 10^{-06}$	$27{,}5 \times 10^{-06}$

Whereas the greater head pressure (and thus pressure drop) generated with nitrogen works to induce a greater flow than in the case of hydrogen, the larger nitrogen viscosity works to reduce the flow compared to the case of hydrogen. Nonetheless, the recycle ratio obtained for nitrogen is substantially greater than that for hydrogen as the increase in pressure considerably outweighs the counteracting effect of larger gas viscosity and, hence, the findings presented in Figures 6.2 – 6.6.

With regard to temperature, the results presented in Section 6.2.2 show that the recycle ratio decreases with an increase in temperature. This may be attributed to the fact that an increase in temperature results in a decrease in the gas density and, consequently, a decrease in the pressure head (and thus pressure drop) generated, which induces a lower recycle flow. The relative magnitudes for the pressure drop delivered at various temperatures for nitrogen, as determined using the calculations presented in Appendix IV, can be viewed in Table 6.3.

Table 6.3: Change in pressure drop over catalyst bed with temperature for nitrogen

Temperature	Pressure drop
25℃	540 Pa
100℃	414 Pa
200℃	327 Pa

In addition to the decrease in density, the increased temperature also results in an increase in gas viscosity as shown in Table 6.2. Consequently, at constant overall pressure in the reactor, increasing the temperature effects a decreased pressure head (and reduced pressure drop over the bed) and an increased gas viscosity, both of which serve to induce a lower flow through the catalyst bed, resulting in the recycle ratios decreasing with an increase in temperature.

6.3.2 Effect of catalyst mass on recycle ratio

A powdered FT catalyst with a size distribution of 25 – 250 μm was used in the RTD experiments. This size fraction is representative of that used in HTFT synthesis in fluidized bed reactors. Smaller catalyst particles are preferred for reactions as they offer a larger particle effectiveness factor, however, at the expense (often limiting) of a larger pressure drop. Hence catalyst particles sizes are chosen as an economic compromise between activity and pressure drop.

The effect on recycle ratio of using such a fine powdered catalyst was investigated. From the results presented in Figure 6.9, it is inferred that the addition of catalyst or in fact the amount of catalyst used does not contribute significantly to the pressure drop as is evidenced by the small drop in recycle ratio with and increase in catalyst loading. The recycle ratios fall within 10% of each other (for no catalyst and loadings of 5 g and 10 g respectively), thus demonstrating that the pressure drop generated across the catalyst bed is predominantly due to the felts, with the fine powdered catalyst only contributing marginally.

Although the impact of the catalyst loading is more pronounced at higher pressures, the influence of catalyst loading remains a secondary effect on recycle ratio throughout the useful operating range of the STIRR.

6.3.3 Effect of syngas composition

In light of this STIRR finding its place for the use of catalyst testing for Fischer-Tropsch synthesis, the recycle ratio for various compositions of CO and H_2 (which make up the Fischer-Tropsch feed gas) was determined.

The recycle ratio decreases with increasing molar fraction of hydrogen in the mixture, consistent with the earlier findings (Section 6.3.1) in respect of decreasing gas density and viscosity. At a ratio of H_2/CO of 2, ubiquitous in Fischer-Tropsch synthesis, the recycle ratio is approximately half of that with pure CO. in the case of a true FT experiment, as the reaction proceeds, the conversion of syngas to higher hydrocarbons and water will increase the density and viscosity of the mixture as the partial pressure of hydrogen is lowered and, therefore, the recycle ratio is expected under reaction conditions to be higher than that for the pure syngas feed.

6.3.4 Recycle flow under HTFT conditions

High Temperature Fischer-Tropsch reactions are run at a temperature and pressure in the region of 300℃ and 20 bar, respectively. The recycle ratio obtained at these conditions using nitrogen as the feed gas was found to be 37 at an impeller speed of 960 rpm.

From the result of the effect of a syngas composition on recycle ratio (Figure 6.10), it can be seen that when using a syngas feed mixture of H_2/CO of 2 (as commonly used in FT synthesis experiments), a recycle ratio of 30 is obtained. This is just over 50% of the recycle ratio of 55 obtained when pure CO feed gas is used. Noting that nitrogen and carbon monoxide have the same density (molecular mass), if a recycle ratio of 37 is achieved using a pure nitrogen feed, then based on the findings of Figure 6.10, it can be deduced that when using a syngas feed mixture of H_2/CO of 2, a recycle ratio of just over 50% (approximately 20) should be obtained.

As explained in the previous section (Section 6.3.3), as the FT reaction proceeds, products with a higher density and viscosity are formed, thus resulting in a prevailing mixed gaseous environment for which the impeller will induce an even greater flow and recycle ratio. Furthermore, it must also be noted that for this experiment a fairly low impeller speed of 960 rpm was employed. Laboratory scale HTFT experiments performed in an STIRR reactor are usually performed at impeller speeds in excess of 1500 rpm thereby ensuring a substantially greater recycle ratio.

Thus, even taking into consideration that the result may be over-estimated by a maximum of 25%, the resulting recycle ratio will remain greater than the minimum required recycle ratio of 20 required to classify the reactor as a CSTR.

7. Conclusions

Keeping the objectives of this study in mind, the following principal conclusions can be drawn:

- The novel arrangement of positioning the inlet and outlet capillaries in close proximity of each other ensures that the tracer recycle peaks in RTD studies can be clearly distinguished before the methane disperses into the feed gas thus enabling the calculation of the recycle ratios. Furthermore, an increased range of measurability for the recycle ratios can be achieved with the capillaries in this arrangement.

- Previous studies performed by Prinsloo and Koning (2005) were unable to establish a clear correlation between the impeller speed and recycle ratios, possibly allowing for the interpretation of insufficient gas flow through the catalyst bed. From the experiments performed during this study, the results clearly indicate that not only is the STIRR well mixed but that this is as a result of a high recycle flow through the catalyst bed, thereby ensuring adequate gas-catalyst contact. Sufficiently high recycle ratios can be obtained in an STIRR in spite of the catalyst being a very fine powder and the associated catalyst basket design (including metal sieve plates, felts and catalyst) having a high flow resistance.

  Moreover, given that recycle flow through the catalyst bed has been demonstrated, it can be concluded that the expected underestimation of adiabatic temperature increase across the catalyst bed, which was used to determine recycle ratios in the study by Prinsloo and Koning (2005), is not be due to abnormal flow patterns as suggested in Fig.2.10, but rather due to a substantial loss in adiabatic heat of reaction via intimate contact of the catalyst with the highly conductive felts.

- Even under HTFT conditions, it can be deduced that a recycle ratio in excess of 20, the minimum required value to satisfy the condition of negligible concentration and temperature gradients, can readily be achieved in the STIRR under HTFT conditions making it suitable for the purpose of HTFT catalyst testing.

References

Bathie, W.H., *Fundamentals of Gas Turbines*, John Wiley and Sons Inc (1984)

Berty, J.M., *Reactor for Vapour-Phase Catalytic Studies*, Chemical Engineering Progress, 70(5), pp. 78-84 (1974)

Berty, J.M., *Testing Commercial Catalysts in Recycle Reactors*, Catalysis Reviews, Sci. Eng, 20(1), pp 75-96 (1976)

Berty, J.M., *20 Years of Recycle Reactors in Reaction Engineering*, Plant/Operation Progress, 3(3), pp 163-168 (1984)

Botes, F.G., *The addition of HZSM-5 to the Fischer-Tropsch process for improved gasoline selectivity*, MSc Thesis (Chemical Engineering), University of Cape Town, (2002)

Carberry, J.J., *Designing Laboratory Catalytic Reactors*, Industrial and Engineering Chemistry, 56(39) pp 39-46 (1964)

Carman, P.C., *Flow of Gases through Porous Media*, Butterworh Scientific publications, Chapter 3, pp182 (1956)

Danckwerts, P. V., *Continuous-flow systems. Distribution of residence times***,** Chemical Engineering Science, 2 pp 1-13 (1953)

Fogler, H.S., *Elements of Chemical Reaction Engineering*, Prentice Hall International Inc., Chapter 8 (1999)

Gillespie, B. and Carberry, J.J., *Influence of Mixing on Isothermal Reactor Yield and Adiabatic Reactor Conversion*, I & EC Fundamentals 5(2) pp 164-171 (1966)

Levenspiel, O., *Chemical Reaction Engineering*, John Wiley and Sons Inc, Chapter 9 (1962)

MacMullin, R.B. and Weber, M., *Determining the efficiency of continuous mixers and reactors*, Chemical and Metallurgical Engineering, 42 pp 254-257 (1935)

Melo, A.P., Pinto, J.C. and Biscaia Jr., E.C, *Characterization of the residence time distribution in loop reactors*, Chemical Engineering Science, 56, pp 2703-2713 (2001)

Möller, K.P., Fletcher J.C.Q., O'Connor, C.T. and Becker, R.J., *Residence Time Distribution in a Jetloop Reactor*, Chemical Engineering Communications, 137, pp 111-118, (1995)

Perry, R.H. and Chilton, C.H., *Chemical Engineer's Handbook*, 5th Edition McGraw-Hill, (1973)

Prinsloo, F. and Koning, B., *Development and Testing of a Stirred-from-Top Berty Micro reactor*, Internal report, Chemicals from Synthesis Gas Group, Research and Development, Sasol (2005)

Prinsloo, F., Chemicals from Synthesis Gas Group, Research and Development, Sasol, Personal Communication (2007)

Rippin, D.W.T., *The Recycle Reactor as a Model for Incomplete Mixing*, I & EC Fundamentals, 6(4), pp 488-492, (1967)

Schermuly, O. and Luft, G., *Studies on low-pressure methanol synthesis in a jet reactor,* Chemie Ingenieur Technik 49(11), pp 907 (1977)

Smith, J.M., Van Ness, H.C. and Abbott, M.M., *Introduction to Chemical Engineering Thermodynamics*, 7th Edition, McGraw-Hill (2005)

Schwan, P., Transport *Analysis of Diffusion and Adsorption under Reaction Conditions*, MSc Thesis (Chemical Engineering), University of Cape Town, (2001)

APPENDICES

Appendix

Appendix I – Pictures of reactor and reactor test unit

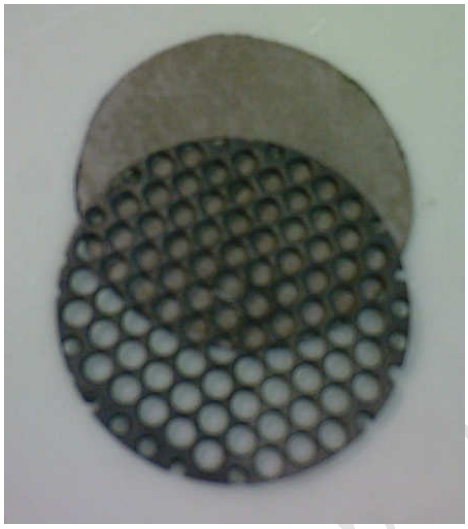

Figure A1.1: Photograph of felt and metal sieve plate

Figure A1.2: Photograph of internal draft tube with felts and metal sieve plates

Figure A1.3: Photograph of reactor base, internal draft tube, felts and metal sieve plates

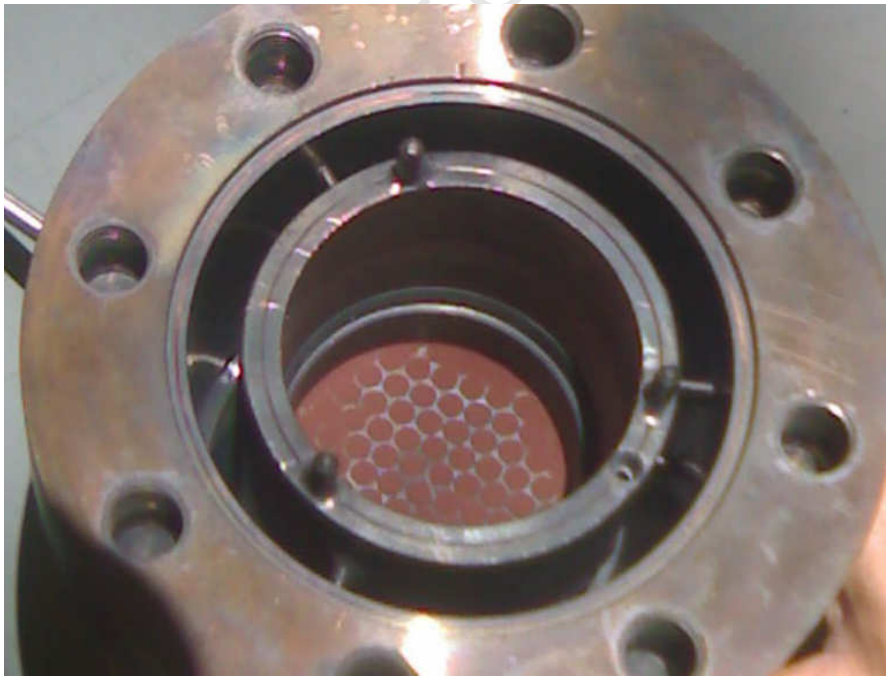

Figure A1.4: Photograph of reactor with internal draft tube in place showing catalyst neatly filling holes of metal sieve plate

Figure A1.5: Photograph of closed reactor with magnedrive impeller

Figure A1.6: Photograph of reactor base and lid with impeller

Figure A1.7: Photograph of reactor test unit

Appendix II – Experimental lists

Table A2.1: Parameters investigated for experimental study

Gases	N_2
	H_2
	CO
Internal configuration	0 Felt
	1 Felt
	2 Felts
Capillary position*	Position 1
	Position 2
Temperature	25℃
	100℃
	200℃
	300℃
Pressure	10 bar
	20 bar
	30 bar

Each of these parameters was tested at varying impeller speeds ranging from 250-2500rpm. The gas flow rate was kept constant at **1500 sccm**

Table A2.2: List of experiments performed in method development study

Temperature: 25℃
Pressure: 10 bar
Gas flow rate: 1500 sccm

	Gas	Internal components	Capillary position
Exp 1	N_2	0 Felts	Position 1
Exp 2	H_2	0 Felts	Position 1
Exp 3	N_2	1 Felt	Position 1
Exp 4	H_2	1 Felt	Position 1
Exp 5	N_2	2 Felts	Position 1
Exp 6	H_2	2 Felts	Position 1
Exp 7	N_2	1 Felt	Position 2
Exp 8	N_2	2 Felts	Position 2
Exp 9	H_2	2 Felts	Position 2

For all experiments the impeller speed was varied from 720rpm – 2000rpm.

Table A2.3: List of experiments performed in method development study

	Gas	Pressure	Temperature	Catalyst Mass
Exp 10	HYDROGEN	10 bar	25℃	5 g
Exp 11			100℃	
Exp 12			200℃	
Exp 13			300℃	
Exp 14		20 bar	25℃	
Exp 15			100℃	
Exp 16			200℃	
Exp 17			300℃	
Exp 18		30 bar	25℃	
Exp 19			100℃	
Exp 20			200℃	
Exp 21			300℃	
Exp 22	NITROGEN	10 bar	25℃	
Exp 23			100℃	
Exp 24			200℃	
Exp 25			300℃	
Exp 26		20 bar	25℃	
Exp 27			100℃	
Exp 28			200℃	
Exp 29			300℃	
Exp 30		30 bar	25℃	
Exp 31			100℃	
Exp 32			200℃	
Exp 33*	SYNGAS	20 bar	25℃	
Exp 34	NITROGEN	10 bar	25℃	0 g
Exp 35				10 g
Exp 36		20 bar		10 g

* Impeller speed constant at 720 rpm, composition of syngas varied

All experiments were performed with a feed gas flowrate of 1500 sccm, 2 felts in place and with inlet and outlet capillaries in position 2. The impeller speed was varied from 720 rpm – 2000 rpm, unless otherwise indicated.

Appendix III – Quadratic trend lines

The data presented in the figures are fitted with quadratic trend lines suggesting the existence of a quadratic relation between the recycle flow velocity and the impeller rotational speed. From the literature review it can be understood that the energy transferred to the gas as work done on the gas is consumed to increase the enthalpy of the gas – which raises the static pressure – and the kinetic energy of the gas – which can be understood as dynamic pressure – in almost equal parts. Equation $W_{\tan} = u_2 v_{u_2} - u_1 v_{u_1}$ and $W_{axial} = \frac{v_{a_2}^2}{2} - \frac{v_1^2}{2}$ and combining $W_{\tan}$ and W_{axial} to give W_s show that the work done on the gas depends on the square of the impeller rotational speed. The generated velocity head driving the gas through the bed equals the velocity head offered by the resistance to flow through the bed. It will be explained in the discussion that the latter is proportional to the viscosity of the gas and to the velocity of the gas in a linear way.

$$\frac{\Delta p}{L} = au + b\rho u^2$$

Thus, by equating the generated pressure head which displays a square dependency on impeller speed to the pressure drop over the bed which depends linearly on the velocity of the gas through the bed, it can be concluded that a quadratic relation exists between the velocity of the recycle flow and the impeller speed.

Appendix IV – Pressure drop calculations

The following equations were used to calculate the pressure drop over the catalyst bed. The velocity diagram of the internal flow and its influences within the reactor is presented in Figure A.1. The discussion on the theory behind the calculation can be found in Section 2.3.

P = 1,00·10^6 N/m^2
T = 298 K
Q_{in} = 1500 ml/min (STP)

d_{blade} = 7,00 cm
d_{shaft} = 1,00 cm
r_{ave} = 2,00 cm

v = 1920 rpm
u = 4,02 m/s
k = $C_{p,m}/C_{V,m}$ = 1,40

$$T_{t_1} = T_1 + \frac{v_1^2 M}{2c_p}$$

$$T_{t_2} = T_{t_1} + \frac{W_{\tan} M}{c_p} + \frac{W_{axial} M}{c_p}$$

$$T_{t_2} = T_1 + \frac{u v_{u_2} M}{c_p} + \frac{v_{a_2}^2 M}{2c_p}$$

Table A4.1. Pressure drop calculation for nitrogen and hydrogen

	N_2	H_2
M (kg/kmol)	28	2
$C_{p,m}$ (kJ/kmol K)	29,125	28,824
$\dot{m}_{in}$ (kg/s)	2,82·10^{-5}	2,02·10^{-6}
R = measured recycle ratio	117	26
v_1 (m/s)	7,63·10^{-2}	1,66·10^{-2}
β_1 (°)	88,9	89,8
v_{u_2} (m/s)	3,94	4,00
W_s (J/kg)	23,95	24,19
$\frac{P_{t_2}}{P_{t_1}} = \left(\frac{T_{t_2}}{T_1}\right)^{k/k-1}$ $\Delta P = P_{t_2} - P_{t_1}$ (Pa)	270	20

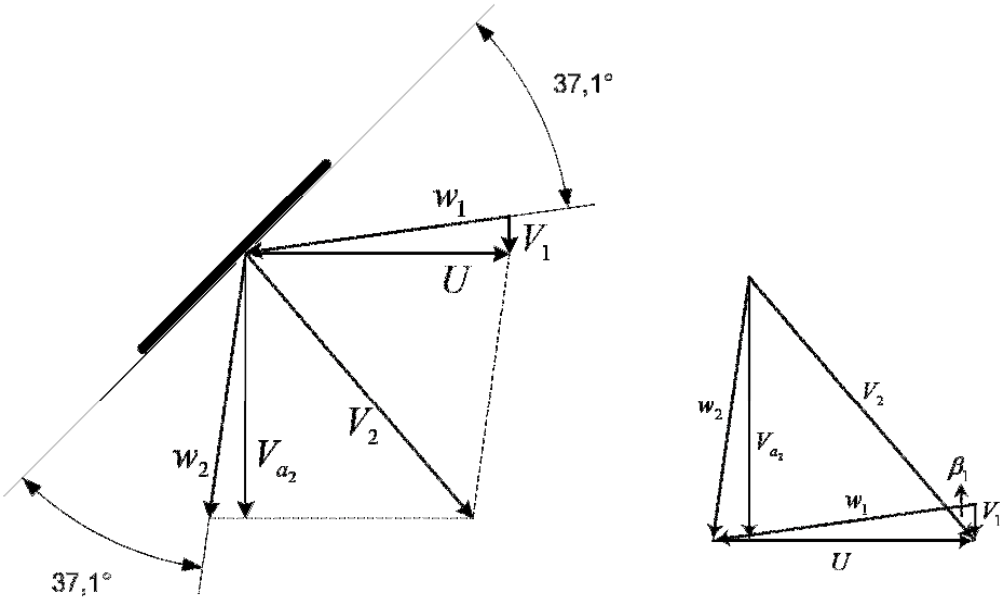

Figure A4.1: Velocity diagram of the internal flow and its influences within the reactor